Chapter -4 Carbon Sequestration to Mitigate the Impact of Climate Change

Chapter · December 2022

DOI: 10.22271/int.book.196

CITATIONS
0

READS
42

1 author:

Ferooze Ahmad Rafiqi
Government Degree College Anantnag
21 PUBLICATIONS **141** CITATIONS

SEE PROFILE

ADVANCES IN CHEMICAL SCIENCES

Volume - 4

Chief Editor

Dr. Anurika Mehta
Associate Professor, Poornima Institute of Engineering Technology, Jaipur, Rajasthan, India

Co-Editor

Dr. Simanchal Das
Assistant Professor, Roland Institute of Technology, Berhampur, Odisha, India

Integrated Publications
New Delhi

Chapter - 4

Carbon Sequestration to Mitigate the Impact of Climate Change

Authors

Dr. Ferooze Ahmad Rafiqi
Assistant Professor, Govt. Degree College Anantnag,
Department of Higher Education, Jammu and Kashmir, India

Shabir Ahmed Bhat
Assistant Professor, Govt. Degree College Anantnag,
Department of Higher Education, Jammu and Kashmir, India

Raveed Yousuf Bhat
Assistant Professor, Govt. Degree College Anantnag,
Department of Higher Education, Jammu and Kashmir, India

Chapter - 4

Carbon Sequestration to Mitigate the Impact of Climate Change

Dr. Ferooze Ahmad Rafiqi, Shabir Ahmed Bhat and Raveed Yousuf Bhat

Abstract

In this study, carbon sequestration methods and technologies were exhaustively analyzed and comparative assessment of the materials and processes were evalvated for carbondioxide removal capacites. Layer Double Hydoxides, Layered Doubles Oxides, Intercalated Double Hydroxides have shown limited CO_2 sequestration potentials. The oxides of Mg, Ca and transition metals on account of their favourable temperature window and basic character of oxide ion (O^{2-}) find applications in CO_2 sequestration technologies such as adsorption, calcium looping and chemical looping processes. Based on the current state of art in the field of CO_2 absorption technologies, amine based solvents, novel solvents, blends and ionic liquids have shown an excellent and remarkable performance in the CO_2 separation Processes. Metal Organic Frameworks (MOFs) are attractive candidate for CO_2 removal purposes. These materials can be made more competitive with the modifications of basic MOF structure like amine functionalization, haterocyclic ring insertion and incorporation of open Metal Sites (OMS). The results of the study of these perspective materials for CO_2 sequestration applications would give a new insight and understanding for developing carbon efficient devices and methods in pollution control and mitigation policies.

Keywords: Carbon sequestration; CaO; MOF; thermal stability, adsorption, absorption, carbondioxide.

1. Introduction

Carbondioxide and Water vapor in air moderates and regulates the temperature of the earth but the anthrophogenic emission of greenhouse gases has disrupted the carbon cycle and thus accelerated the global warming. Augementing the percentation of CO_2 in the atmosphere due to anthropogenic activity has increased the average temperature of the earth

thereby making this blue planet vulnerable to several issues like cyclones, droughts, floods, coastal erosion, and many more phenomena. This is the scenario unfolding at present. The devastative effects of climate change were reported in the past [2-4], noticed even today [5] and will happen in the future too provided the requisite steps would not be taken to mitigate the adverse impacts of climate change. Many people who contributed no or little greenhouse gas emissions are also vulnerable to climate change. As per the Global Climate Risk Index 2020 and the analysis based on the impacts of extreme weather events and the socio-economic losses, the most affected places by climate change today are Japan, Germany, Madagascar, Canada, India, Fiji, Maldives, Sri Lanka, Kenya, Zimbabwe and Ruanda [6, 7]. Some areas are drought prone and some are vulnerable to floods. There are regions where there is food insecurity and in certain areas of the world water is contaminated and of low quality, thus such areas have health risk concerns. By 2050, population will touch 9 billion from 7 billion [8]. Energy demand is also expected to increase by 50% over the next 2 decades. To meet out the energy demands of such a huge population, it is largely met by burning fossil fuels. Simultaneously mitigating climate change and fulfilling energy demands of the world is a tremendous paradox of the century. To satisfy both the criteria, carbon capture seems to be the mandatory technology for the development of sustainable energy infrastructure.

Fossil fuels represent 80% of the global energy supply and renewable sources constitute merely 13% of the total energy supply. If the world will focus on exploration and harnessing of renewables sources, it could make upto 30% of the global energy supply by 2030 [8-14]. Still we have to rely on fossil fuels and it shall remain the main source of energy for decades to come. Keeping this aspect in view, it can be said that the complete substitution of fossil fuels by the clean energies is extremely difficult. Till the industrial revolution, anthropogenic carbon production mainly from the burning of wood and other sources were balanced with natural carbon capture processes e.g. photosynthesis and ocean atmosphere carbon flux. However, after the advent of the industrial revolution, the situation altogether changed. It is estimated that since then 15-40% increment of anthropogenic CO_2 emissions occurred in the atmosphere [8-14]. Natural processes cannot remove this inordinate CO_2 from the atmosphere alone without the resort of any technology. Keeping this problem in view, it was keenly felt that the exploration of innovative techniques and efficient methods to sequester the excess CO_2 stored in the atmosphere are inevitable. Among the greenhouse gases, CO_2 is believed to be the main cause of

current climate change [15-19]. This has compelled the humans to explore boundless technological options to reduce the CO_2 emissions in the atmosphere. Among the viable technological options available, carbon sequestration is the most promising and mature technology till date.

In this study, Materials like Layer Double Hydoxides, Layered Doubles Oxides, Intercalated Double Hydroxides, Chemical absorption solvents, Solvent blends, Ionic liquids, Porous Carbons, Metal Organic Framework (MOFs) were assessed for carbondioxide capture potentials. Strategies for improving the CO_2 capturing performance by MOFs were also proposed. Besides Carbon Capture and Storage (CC&S) technology, some other methods like Direct Air Capture, Enhanced Weathering, Ocean Acidification neutralization methods, Enzymatic Carbonic anhydrase and cryogenic methods for CO_2 separation were also briefly discussed. Some possible solutions to this burning issue of climate change were proposed.

1.1 Carbon sequestration

It is the process of capturing and storing atmospheric CO_2. It reduces the amount of CO_2 in the atmosphere with the goal of reducing the global climate change. Biologically CO_2 is sequestered through vegetation like grasslands or forests. The storage can occur both in soils and oceans. CO_2 is captured naturally from the atmosphere through physical, chemical and biological processes. Similar effects are being produced through the designing of artificial processes. Naturally CO_2 is sequestered through wetland restoration, peat bogs, reforestation, agricultural practices etc. [3, 20, 21]. CO_2 is also dumped in underground geological formations or rocks. Human Induced Sequestration is carried out by iron fertilization, urea fertilization, carbon capture and storage (CC&S), biochar, subterrain injection [22, 23]. Adding urea or iron compounds (iron sulphates, iron supplements, iron chelates etc.) as fertilizer encourages carbon-munching phytoplankton in extracting CO_2 from the atmosphere.

1.1.1 Direct air carbon capture, enhanced weathering, ocean acidification

Besides the above mentioned techniques, Direct Air Carbon Capture and Storage (DACCS), enhanced weathering and enhanced marine alkalinity has also pressed into service for carbon capturing purposes [24-27]. CO_2 in the atmosphere is so scarce and to remove it directly from the atmosphere is very energy intensive and highly expensive. It is present in the concentration of a few hundred parts per million.

Weathering is the breaking down of rocks and minerals in-situe. The

agents that enhances the disintegration of rocks are natural forces like wind, water, ice, plants and animals. Climate affects the weathering phenomenon. The rocks that are exposed to heavy rains and humidity and received a scorching heat crumbled faster than the rocks located in the dry and cold climatic conditions. The rocks found in equatorial climates undergo fast weathering than located in polar regions.

Enhanced weathering is induced weathering in which finely ground silicate rock such as basalt is poured onto surfaces that speeds up reaction between water, air and rocks. Weathering removes CO_2 as carbonic acid. The dissolved CO_2 solution is in equilibrium with the atmospheric CO_2. The CO_2 that was lost due to weathering made the rock deficient of carbon. This deficiency is overcomed when more CO_2 is removed from the atmosphere. The ocean acidification can be abated and counteracted as the enhanced weathering turns water more alkaline.

The oceans absorb nearly one third of anthropogenic CO_2 emissions acting as the largest carbon sinks on the earth. With the increase in the CO_2 concentration in the atmosphere, the oceans absorb more quantity of it thereby making the ocean water more acidic. At low water pH, the ability of some marine organism like coral reefs, shellfish and some phytoplankton plants to form shells and skeltons drops. Coral bleaching is caused by ocean warm waters. Coral bleaching together with ocean acidification cause untold damage to coral reefs. The intensity and severity of tropical storms as a result of climate change are less devastative and calamitous when coral reefs are plenteous in the oceans. These coral reefs act as buffers to tropical storms. The only thing that can obviate the coral reefs to undergo destruction is to increase the alkalinity in the ocean water.

1.1.2 Carbon Capture and Storage (CC&S)

Carbon Capture and Storage (CC&S) is a three tier process. It involves; 1) Capturing CO_2 at large and stationary point sources 2) Transporting the CO_2 from source to sink and 3) Injecting the CO_2 in suited geological reservoirs or sinks.

Thus, CCS technology allows the transport of galore CO_2 from the point source to safe underground reservoirs thereby avoiding the release of CO_2 into the atmosphere. CCS is therefore an important climate protection technology [4, 24].

The three systems operated in CCS technology for the separation of CO_2 from the flue gas are pre-combustion, Oxy fuel combustion and post combustion processes, schematically shown in Figure 1 [25].

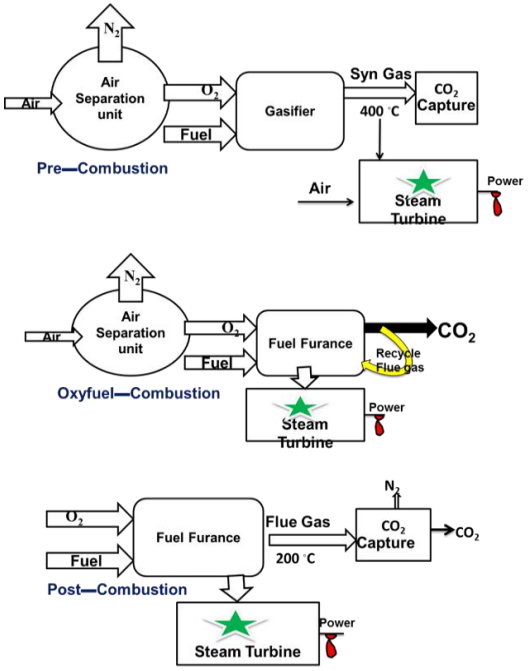

Fig 1: Schematic Diagram of Pre-combustion, Oxy-fuel combustion and post combustion processes

CO_2 is separated from the flue gas before combustion in pre-combustion process. The fuel is then converted to syn gas (30-60% CO, 25-30% H_2, 5-15% CO_2 and 0-5% CH_4) [23].

Oxy fuel combustion uses pure oxygen instead of air so it increases the heating system efficiently. It produces CO_2 and H_2O only thereby obviating the further separation of exhaust gases. CO_2 gas produced can be directly captured. Air contains maximum percentage of N_2 that can dilute the reactive O_2 in the combustion of fuels.

Separation of CO_2 is easier in the post combustion process on account of availability of the methods like adsorption, absorption, membrane separation, cryogenic method and the enzymatic carbonic anhydrase method [28, 29]. Carbonic anhydrase is a natural fast biocatalyst. It carries CO_2 from the tissues to the lungs. The use of Carbonic anhydrase in the industries for the CO_2 removal proved fruitful only at low temperature conditions. At high temperature, the enzyme undergoes protein denaturation making it less effective and thus hinders its commercial applications. Cryogenic method is also an innovative CO_2 capture option. It has the potential of removing 90-95% CO_2 emissions from fossil fuel based plants. The main hurdle to use

this method on commercial lines is to convert CO_2 into liquid form under cryogenic conditions that is a very difficult process and thus it is less efficient.

CCS status in the world is very poor. If the targets laid out by the Intergovernmental panel on climate control (IPCC) are to be met out then the world ought to increase the carbon capture at least 100 fold by 2050. It is in place to mention here that global storage capacity has increased 32% in the year 2021 as per the global status CCS report of 2021 [1].

1.2 Materials used as carbon sequestrants

1.2.1 Layer double hydoxides, layered doubles oxides, intercallated double hydroxides: These hydoxide compounds have been used as carbon sequestrants. Their general formula is M^{2+} = (Mg^{2+}, $Cu^{2+,}$ Zn^{2+}, Ni^{2+}or Mn^{2+}); M^{3+} = (Al^{3+}, Cr^{3+} or Fe^{3+}), A^{n-} = (CO_3^{2-}, SO_4^{2-}, NO_3^-, Cl^- or OH^-) For Example: $(Mg)_{1-x}Al_{(x)}$ $(OH)_2(CO_3)_{x/2}$ mH_2O: Mg-Al-CO_3 layered Double Oxide [30].

Due to poor basic strength and presence of charge compensating anions make these compounds less efficient towards CO_2 adsorption. However, such compounds during calcination undergo structural transformation into three dimensional network of amorphous mixed metal oxides referred as layered double oxides.

Layered double oxides show good hydrothermal stability, high selectivity of CO_2 capturing ability and high regeneration capacity.

Intercallation of organic anions such as carboxylates and dicarboxylates in Layered double hydroxides improves their adsorption properties. Such intercallated Layered Double Hydroxides when subjected to thermal treatment change into more disordered microstructures resulting in enhanced surface basic sites besides developing amorphicity [30]. This improved their CO_2 capture properties further.

1.2.2 Metal oxides: The oxides of Mg, Ca and transition metals find applications in CO_2 sequestration technologies such as adsorption, calcium looping and chemical looping processes [31-34].

Mg or Ca provides basic sites (O^{2-}) interacts with Lewis acid CO_2 and form complexes of different nature like carbonates (monodentate, bidentate or bridging), carbonate ions and bicarbonates. Thermal stability of MgO and CaO ranges in the order of 200-500 °C and 500-900 °C, respectivelly. The general reaction between MgO and CaO is represented as:

$MgO + CO_2 \rightarrow Mg{-}O\ldots\ldots..CO_2$ (ads.)

Calcium Looping: The calcium looping cycle is based on the reversible reaction between CaO and CO_2. In the carbonator chamber, formation of calcium carbonate ($CaCO_3$) occurs and in the calciner chamber, decomposition of $CaCO_3$ takes place. The general reaction is shown below:

$CaO(S) + CO_2\ (g) \longrightarrow CaCO_3\ (S)$; ΔH = -175 kJmol

$CaCO_3\ (s) \longrightarrow CaO(s)+CO_2(g)$; ΔH = +179 kJmol

The reactions taking place in the carbonator and calciner are exothermic and endothermic, respectively. Once the flue gas is fed into the carbonator chamber, most of the CO_2 is consumed leaving the unspent flue gas CO_2 free as shown in the Figure 2. CO_2 is then removed from the calciner chamber for storage. This method is cost effective.

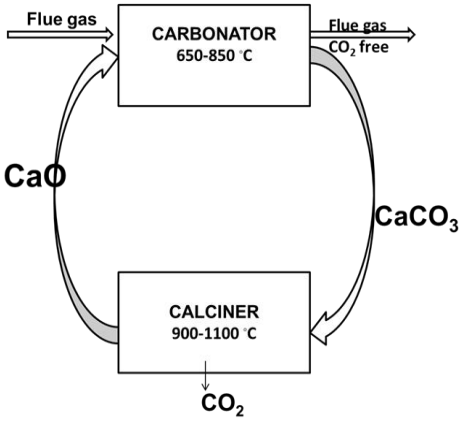

Fig 2: Schematic diagram of calcium Looping cycle

Chemical Looping Combustion Process: In this process, oxygen is produced in-situ eliminating its need to separate from air. In this way, it reduces the system cost and energy expenditure. The general reaction involued in chemical looping is represented as:

$(2n + m)M_xO_y + C_nH_2m \longrightarrow (2n + m)M_xO_{y-1} + mH_2O + nCO$

The experimental setup contains fuel reactor and air reactor as shown in Figure 3. The fuel is introduced into the fuel reactor that contains already an oxide carrier. The major oxygen carrier materials used for chemical looping system are oxides of transition metals like NiO, Fe_2O_3, FeO, CuO, Mn_3O_4 and CoO. Fuel reacts with oxygen carrier inside the fuel reactor. The CO_2 and H_2O produced in the fuel reactor enters into the air reactor where H_2O is condensed out to get pure CO_2 stream for Storage.

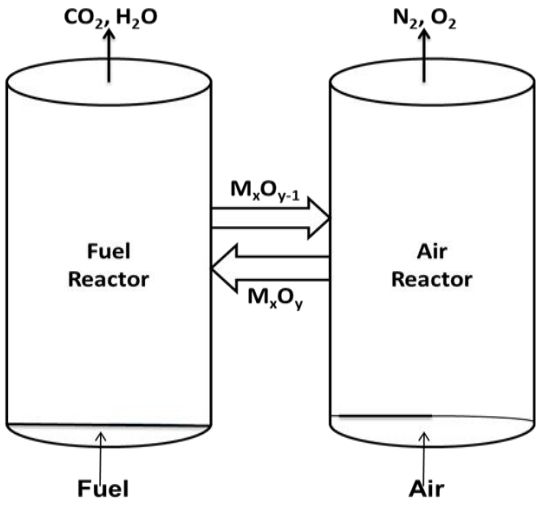

Fig 3: Schematic Chemical Looping Combustion Process.

1.2.3 Solvents used for carbondioxid capture

Post Combustion capture seems to be a mature and proven technology but a little bit expensive. It is result oriented only when novel solvents and optimized processes are used [35-37]. Solvents used for CO_2 capture are of two types; Chemical absorption solvents and Physical absorption Solvents. Physical absorption solvents selectively capture CO_2 in contact with a gas stream without a chemical reaction taking place. Chemically absorption solvents are Conventional amine based solvents, Sterically hindered amine solvents, Non-amine based solvents, solvent blends and Ionic Liquids [38-44]. Physical absorption solvents are Selexol, Rectisol, Ifpexol, Fluor, Purisol, Sulfinol and Morphysorb [37].

Amine Based Solvents: Primary and secondary amines react with CO_2 through zwitterion mechanism form stable carbamates that restricts their additional CO_2 absorption ability. Tertiary amines form bicarbonate ion and protonated amine with CO_2. CO_2 once absorbed can be released by heating the solution in a separate stripping column. The stripping of CO_2 takes place at 120 ℃ [45]. Stearically hindered amines show higher CO_2 adsorption capability than the primary and secondary amines. Introducing a bulky substituent adjacent to amine group lowers the stability of carbamate formed between amine and CO_2 molecule. This weak bond can be easily cleaved, requiring low energy for CO_2 release thereby regenerating the amine functional site for another CO_2 molecule. The general reaction scheme of the CO_2-amine system is represented below:

$$2R\text{-}NH_2 + CO_2 \xrightarrow{Non-Polar\ solvent} RNHCOO^- + RNH_3^+$$

Primary amine Carbamate salt

$$R\text{-}NH2 + CO_2 \xrightarrow{Polar-aportic\ solvent} RNHCOOH$$

Primary amine Carbamic acid

$$HNR_1R_2 + CO_2 \longrightarrow R_1R_2NCOOH$$

Secondary amine

$$R_1R_2R_3N + CO_2 + H_2O \longrightarrow R_1R_2R_3NH^+ + HCO_3^-$$

Tertiary amine Protonated amine

Solvet blends: Solvents bearing functional groups -OH and $–NH_2$/-NH (Monoetnanolamine: MEOA, Diethanolamine: DEOA, Triethanolamine: TEOA etc.) are more attractive in CO_2 scrubbing technology [40, 45-49]. The hydroxyl group serves to reduce the vapour pressure by hydrogen bonding with water and the amino group provides the basic site for acidic CO_2. Thus, such solvent blends serve a duel purpose. They enhances the overall behaviour of the solvents. Some solvent blends are tabulated as shown in Table 1 [41-43].

Table 1: Examples of some Solvent Blends

Solvent	Abbreviation
Piperazine and potassium carbonate	PZ+ K_2CO_3
2-Amino-2-methyl-1-propanol and piperazine	AMP+ PZ
2-Amino-2-methyl-1-propanol and 1,2-ethanediamine	AMP+ EDA
2-Amino-2-methyl-1-propanol and dimethyl-monoethanolamine	MAPA + DMMEA

Ionic liquids: Recently ionic liquids have emerged as a novel solvents for CO_2 capturing purposes. These solvents have replaced the traditional amine based solvents. They solubulize the gases and behave as physical solvents. The CO_2 solubility by ionic liquids are governed by Henry's Law. Some examples of ionic liquids are 1-Butylpyridinium tetrafluoroborate [Bpy] [BF_4], 1-Butyl-3-methyl-imidazolium hexafluorophosphate [bmim] [PF_6], 1-Butyl-3-methyl-imidazolium acetate [bmim] [Ac etc. [38-40, 44].

Ionic Liquids are green solvents in which anions have more impact than cations. For example [bmin] BF_4 is completely miscible with water while as [bmin] PF_6 is largely immiscible with water. The selection of cation and anion makes these ionic liquids tunable or designer solvents. The tunable solvent characteristics allows them to offer unique molecular structures.

Each structure is designed for specific application. Despite ionic liquids show high CO_2 solubility and selectivity for CCS applications but to make them more competitive and functional, amino group incorporation is inevitable. Functionalized ionic liquids like primary and secondary amines form zwitterion with CO_2. Moreover, free space in the ionic liquids are generated due to the asymmetrical structure of the cation and traps the CO_2 molecules easily and efficiently in the free spaces.

1.3.4 Porous carbons, zeolites, metal organic framework (MOFs) for carbondioxide capture

Activated carbon, Graphene oxide, zeolites, carbon nanospheres, porous carbon nanosheets, nanofibres are perspective materials for CO_2 removal on account of the large amount of microporosity with pore diameters of nanoscale range, polar surface emblazoned with hateroatoms like O, N, S species and large surface area [50-61].

Mesoporous silica, zeolites and porous carbons show physiosorption. They require mere 1 bar of pressure at room temperature for CO_2 adsorption. While as Metallic organic framework and Covalent organic framework (COF) exhibit chemisorption and adsorption occurs at 30-50 bar [4]. One fascinating feature that makes these porous materials attractive candidates for CO_2 adsorption is the pore diameter matachability. The kinetic diameter of CO_2 is 3.3°A(0.33 nm) and pore diameter of zeolites, porous carbons, MOF and COF molecules are in the range of 0.4-0.6 nm.

MOFs are composed of two components; metal nodes and organic ligand linkers. The selection of metal and the organic ligand determines the framework structure, surface area and pore volume. The Precedence of MOFs as adsorbents over the other porous carbon materials are because of their large surface area, wide range of structures, design and tenability [62-66]. MOFs can be made more functional with the insertion of amino and carboxylic acid functional groups, insertion of haterocyclic rings and incorporation of open Metal Sites (OMSs) into the pores of metal organic framework [67-69]. The functionalized MOFs are produced either using the amine/carboxylic acid functional ligand during MOF synthesis or post modification synthesis of MOF. Making one or more than one modification in the basic MOF structure enhances the overall capture abilities and storage capacities. MOFs at high pressure has the ability to store 10-12 times more quantity of CO_2 than an empty cylinder. Amine or carboxylate functionalization in MOFs show enhanced selectivity and adsorption capacity primarily due to Lewis acid-Lewis base interactions. OMSs

augment the adsorption capacity of MOFs as the CO_2 moieties get attached at the pore sites where metal ions are available. They bind one another through induction of dipole-quadrupole interactions [70]. Unlike O_2 and N_2, CO_2 has polarizability and quadrupole moment. On account of these factors, they are preferentially adsorbed over N_2 and O_2 by MOFs and MOF like materials. The coordinatively unsaturated metal ions and the presence of high positive charge on the metal ions offers the ideal conditions to attract CO_2 in the adsorption phenomenon. Some examples of MOFs with all the requisites are enlisted here [1, 17, 71-75].

1) 3D Zn(Bmic) MOF [Bmic: benzimidazole carboxylic acid]: It is rich in amino groups and uncoordinatined oxygen atoms. There are multiple open metal sites and imidazole haterocyclic rings.
2) Diamine post-functionalized Mg2(dobpdc) MOF [dobpdc: dioxidobiphenyl dicarboxylate]: There are amine and carboxylic functional groups available and also dioxidobiphenyl haterocyclic rings.
3) $Ni_8(OH)_4(BDP\text{-}COOH)_6$ MOF [BDP-COOH:Boron dipyro methane carboxylic acid]: It is rich in free carboxylate groups besides containing Borondipyromethane rings.
4) M-$BPZNO_2$ (where M= Co, Cu, Zn) [$BPZNO_2$: nitrobipyrazole]: It has pyrazole ring and NO_2 functional group.
5) Mmen-Mg2 (dobpdc): This MOF is produced via post modification synthesis. Mmen stands for dimethylethyl[ene diamine. It is rich in amino groups that enhances its adsorption capacity many times than the parent MOF [76].

Stability of MOFs

1. **Chemical stability:** It describes the resistance of MOFs towards acids, alkalies, water and other solvents. pH is one of the factors that affects the stability of MOFs. MOFs such as MIL-101(Cr) [MIL: Material Institute of Lavoiser], MIL-53 (Al), NH_2-MIL-101(Al), NH_2-UiO [UiO: University of Oslo], UiO-67 and Zeolite imidazole Framework (ZIF-8) are some MOFs that show resistance against air, acid, base or aqueous solutions [65-69, 77-79]. The chemical stability of a MOF containing inert center metal ion is more than containing a reactive central metal ion. Zirconium, an inert metal imparts thermal stability to Zirconium based MOFs against acid and the alkaline aqueous solution of pH 1-9 [80].
2. **Thermal stability:** When a particular MOF is subjected to thermal

treatment, its resistance to undergo breakdown describes its thermal stability. Thus it is the behaviour of MOF towards the heat. MOFs containing stronger node linker bond show resistance to breakdown on exposure to heat treatment [81]. MOFs containing trivalent cations like Fe^{3+}, Al^{3+}, Ti^{4+} are thermodynamically more stable than the MOFs of divalent cations like Zn^{2+}, Cu^{2+} and Co^{2+} because of stronger metal-ligand bond strength [82]. The fluorination process imparts hydrophobic character to MOF surface that in turn increases the hydrothermal stability of the MOFs. Higher hydrothermal stability leads to better adsorption performance of the MOF.

3. **Mechanical stability:** MOFs with inordinate pore number are mechanically unstable. Sometimes mechanical instability of MOFs arise due to removal of pore filling solvents. MOFs with moderate pore number shows comparatively good adsorption performance than with too low or too high pore number [83].

The MOFs have restricted commercial applications as the raw materials used for MOF production are expensive and not easily available. Besides the unavailability and costliness of raw materials, adsorption and desorption costs of CO_2 are high. Moreover, the regeneration of MOFs are also economically expensive [84, 85].

Strategies for improving MOF performance

1. Bottleneck Effect: The bottleneck effect is the pre-confinement of small molecules like water, methyl alcohol, isopropyl alcohol in the pores of MOFs [86]. These molecules partially block the pores of MOFs thereby making the pore diameter in tune with the kinetic diameter of CO_2. This facilitates the packing of CO_2 molecules easier.
2. Functionalization of MOFs: MOFs can be modified during and after their synthesis. Any modification after the MOF synthesis (post synthetic modification of MOF) is done by impregnation method. Using 2-aminoterepthalic acid, free amine groups can be made available in the pores that enhances the adsorption performance of MOF [85]. MOFs can be smartly designed with the proper choice of amine/carboxylate functionalized ligands and the nodes.
3. Introduction of Heterocyclic rings: Hateroatoms (S, N and O) and pi electrons of rings can improve the adsorption capability of MOFs [71, 72, 76].
4. Ozonolysis of Micropores to Mesopores: This process is a

postsyntheic procedure in which one type of ligand is replaced with another type of ligand. These ligands are similar in every respect but they show different reactivity towards ozone. They have same shape, length and reactivity under given conditions [87].

5. Enhancing Chemical, Thermal and Mechanical Stability enhances the overall adsorption behaviour of MOF against CO_2.

1.3 Possible solutions of climate control

There are myraid possible solutions for climate control, some of which are discussed below:

1. Low Carbon Transport Options: The world should switch to Low Carbon Transport Options. Some countries like Hong Kong, China and Singapore have already developed electric tracts and metros that will discourage the use of personal vehicles. Walking and cycling habits can substitute the fuel consumed vehicles thereby help in mitigating the CO_2 release into the atmosphere.
2. Clean Energy and Cleaner Fuel: Whenever a choice is available, clean sources of energy and fuel should be used and should be always on top priority.
3. Developing green technologies for sustainable environment. The world needs to focus on the development of efficient carbon capture and sequestration technologies.
4. Net Zero Emission: Countries and companies need to pledge to go for net zero emissions.
5. Decoupling of economic prosperity from carbon emissions: The world will overshoot all the targets set to date by IPCC and other environmental organizations provided the developed countries would strongly lessen their benchmark per capita emissions and decouple economic prosperity from carbon emissions.
6. Low Carbon growth: It requires political commitment from all the nations for a sustained structural economic change. Until the countries will not take on this issue on prioritized basis, the world would pay the piper and the battle against the climate change will be lost.
7. Market Oriented Climate Policies: It is a control approach to mitigate the climate change. It imposes pollution charges and enforces marketable permits. It is also called a cap and trade system. It sets a cap or a specific target on the total carbon

emissions. It will encourage private businesses to invest in fossil fuel alternatives. Tax –based regulatory system will avarice the polluters in the form of incentives to explore cost effective solutions to emissions control. Firm who will exceed the emissions beyond the permissible limit has to pay the tax and that which will reduce the emissions can evade the tax.

8. Trade-off among desirable properties while developing a strategy is must: There has been observed an enhancement in the CO_2 capturing property by using an inert support material but simultaneously it has enlarged the reactor size thereby increasing the operational expenditure [33]. Thus, the product cost, human health risk assessment and environmental concerns need to be considered while developing a strategy. Hence material and process development should progress coherently for the successful deployment of CO_2 capture and storage technology.

1.4 Future scope

Researchers are pondering the question of what would be done after the CO_2 storage. CO_2 can be used as a resource and its conversion into high efficient energy fuels is also reported [1, 88-91]. CO_2 has been used in the production of urea, methanol, ammonia and value-added chemicals [92, 93]. Recently CO_2 was used in the Graphene production [94]. Graphene is used in smart phone screens and other tech devices.

Conflicts of interest

There are no conflicts of interest to declare.

References

1. Global Carbon Capture and Storage - Status Report 2020, Global CCS Institute, 2021, https://www.sustainablefinance.hsbc.com
2. Atmospheric effects of air pollution during dry and wet periods in Sao Paulo, Environmental sciences, atmospheres. 2022;2:215-229.
3. Richard Derwent G *et al*. Natural greenhouse gas and ozone depleting substance sources and sinks from the peat bogs of Connemara, Ireland from 1994-2020, Environmental sciences, atmospheres. 2021;1:406-415.
4. Soroush Neyestane E, Rawad Saleh. Observationally constrained representation of brown carbon emissions from wildfires in a chemical transport model, Environmental sciences, atmospheres. 2022;2:192-201.

5. Indri Susanti. Technologies and Materials for Carbon Dioxide Capture, Science Education and Application Journal (SEAJ). 2019;1(2):84-97.
6. Eckstein D, Kunzel V, Schafer L, Winges M. Global Climate Risk Index, 2020, GERMANWATCH e.v., www.germanwatch.org/en/cri
7. The World Population Prospects: The 2017 Revision. published by the UN Department of Economic and Social Affairs https://www.un.org/en/desa/world-population.
8. Robert Rapier, Fossil Fuels Still Supply 84 Percent of World Energy — and Other Eye Openers, Energy, 2020 www.forbes.com.
9. EESI (Enivironmental and Energy Study Institute, Fossil fuels, 2020, https://www.eesi.org/topics/fossil-fuels/description.
10. United in 2021, A multi-organization high-level compilation of the latest climate science information,World Meterological Organization (WMO), 2021.
11. IanTiseo, Annual global emissions of carbon dioxide 1940-2020, statista, Energy and Environment, 2022, https://www.statista.com/markets/408/energy-environment.
12. Masao Gen *et al*. Particulate nitrate photolysis in the atmospheres, Environmental sciences, atmospheres. 2022;2:111-127.
13. Carbon Footprint by country 2022-Emissions Database for Global Atmospheric Research- European Comission Joint Reseach Center, https://worldpopulationreview.com.
14. David Dah-Wei Tsai, Paris Honglay Chen, Rameshprabu Ramaraj. The potential of carbon dixide capture and sequestration with algae, Ecological Engineering. 2017;98:17-23.
15. Bao Z, Li Q *et al*. Innovative cyclic reaction mechanisms of CO_2 absorption in aminoacid salt solvents,Chemical Engineering Journal Advances. 2022;10:100250-260.
16. Jaime Gonzatez, Nathalia Tejedor-Flores, Reinhardt Pinzon. A Bibliographic review of the Importance of carbondioxide in Mangroves, 7th International Engineering, Sciences and Technology Conferences (IESTEC), 2019, DOI: 10.1109/IESTEC46403.2019.00-89.
17. Joris Koornneef, Toon van Harmelen, Arjan van Horssen, Andrea Ramirez. Carbon Dioxide Capture and Air Quality, InTech, Chapter, 2011, 18-44. DOI: 10.5772/18075·

18. Ghosh *et al*. Metal Organic Frameworks for Carbon Capture and Energy, ACS Symposium Series, American Chemical Society, 2021, 201-238.

19. Mengpin Ge, Johannes Friedrich and Thomas Damassa, 6 Graphs Explain the World's Top 10 Emitters (Climate), 2014, world Resources Institute, https://www.wri.org/insights/6-graphs-explain-worlds-top-10-emitters.

20. Sandeep K, Snehesh S, Dasappa S. Carbondioxide Capture Through Biomass Gasification, Conference Paper, 2021.

21. Erdal Sakin, Emrah Ramazanoglu, Ali Seyrek. Effects of Different Biochar Amendments on Soil Enzyme Activities and Carbondioxide Emission, Communications in Soil Science and Plant Analysis, 2021. DOI: 10.1080/00103624.2021.1971694.

22. Abarasi Hart, Helen Onyeaka. Eggshell and Seashells Biomaterials for Carbondioxide Capture, Intechopen, Chapter 2020, 1-13. DOI: 10.5772.Intechopen.33870.

23. Wang M, Lawal A, Stephenson P, Sidders J, Ramshaw C. Post-combustion CO_2 capture with chemical absorption: A state-of-the-art review. Chem. Eng. Res. Des. 2011;89:1609.

24. Lackner KS. The thermodynamics of of carbon dioxide. Energy. 2013;50:38.

25. Kumar A, Madden DG, Lusi M, Chen KJ, Daniels EA, Curtin T *et al*. of CO_2 by physisorbent materials. Angew. Chem. Int. Ed. 2015;54:14372.

26. Wang L, Zhao A, Otto Robinius M, Stolten D. A review of post-combustion CO2 capture technologies from coal-fired power plants. Energy Proc. 2017;114:650.

27. Babar M, Bustam MA, Maulud AS, Ali AH. Optimization of cryogenic carbon dioxide capture from natural gas, Materialwiss. Werkstofftech. 2019;50:248-253.

28. Boucif N, Roizard D, Favre E. The Carbonic Anhydrase Promoted Carbon Dioxide Capture, Membranes for Environmental Applications, Environmental Chemistry for a sustainable World 42, Doi: org/10.1007/978-3-030-33978-4_1.

29. Wang Q, Tay H, Zhong Z, Luo J, Borgna A. Synthesis of high-temperature CO_2 adsorbents from organo-layered double hydroxides with markedly improved CO_2 capture capacity. Energy Environ Sci. 2012;5(6):7526-7530. https://doi.org/10.1039/c2ee21409a.

30. Salaudeen SA, Acharya B, Dutta A. CaO-based CO_2 sorbents: a review on screening, enhancement, cyclic stability, regeneration and kinetics modelling. J CO_2 Util. 2018;23:179-199. https://doi.org/10.1016/j.jcou.2017.11.012.

31. Sun H, Wu C, Shen B, Zhang X, Zhang Y, Huang J *et al*. Progress in the development and application of CaO-based adsorbents for CO_2 capture—a review. Mater Today Sustain. 2018;1:1-27. https://doi.org/10.1016/j.mtsust.2018.08.001.

32. Gopalakrishna Bhatta LK, Bhatta UM, Venkatesh K. Metal Oxides for Carbon Dioxide Capture, Inamuddin et al. (eds.). Sustainable Agriculture Reviews. 2019;38:63-83. DOI: org/10.1007/978-3-030-29337-6_3.

33. U.S. Energy Information Administration. International Energy Outlook 2016, 1st ed. Washington: IEA; 2016

34. Chai S, Li Y, Zhang W, He Z. Simultaneous NO/CO_2 removal performance using Ce-doped CaO in calcium looping process: Experimental and DFT studies, Journal of Environmental Chemical Engineering. 2022;10(5):108236.

35. Hammond GP, Spargo J. The prospects for coal-ired power plants with carbon capture and storage: A UK perspective. Energy Conversion and Management. 2014;86:476-489

36. Fernando Vega *et al*. Solvents for Carbondioxide Capture, Intechopen, 2018, Chapter 8, DOI: org/10.5772/itechopen.71443.

37. Zeng S, Zhang X, Bai L, Zhang X, Wang H, Wang J *et al*. Ionic-liquid-based CO_2 capture systems: Structure, interaction and process. Chemical Reviews. 2017;117:9625-9673.

38. Galan Sanchez LM, Meindersma GW, De Haan AB. Kinetics of absorption of CO_2 in amino-functionalized ionic liquids. Chemical Engineering Journal. 2011;166(3):1104-1115.

39. Luo X, Wang C. The development of carbon capture by functionalized ionic liquids, Current Opinion in Green and Sustainable Chemistry. 2013;7:33-38.

40. Cullinane JT, Rochelle GT. Carbon dioxide absorption with aqueous potassium carbonate promoted by piperazine. Chemical Engineering Science. 2004;59(17):3619-3630.

41. Tong D, Maitland G, Trusler MFP. Solubility of carbon dioxide in

aqueous blends of 2-amino-2-methyl-1-propanol and piperazine. Chemical Engineering Science. 2013;101:851-864.

42. Li L, Voice A, Li H, Namjoshi O, Nguyen T, Du YRG *et al*. Amine blends using concentrated piperazine. Energy Procedia. 2013;37:353-369.

43. Zhang X, Dong H, Zhao Z, Zhang S, Huang Y. Carbon capture with ionic liquids: Overview and progress. Energy Environ. Sci. 2012;5:6668.

44. David H, Van Wagener, Gary T. Rochelle, Stripper Configurations for CO2 capture by aqueous monoethanolamine and piperazine, Energy Procedia. 2011;4:1323-1330.

45. Maratun Najiha Abu Tahari *et al*. Application of Octadecylamine-Based Adsorbent on Carbon Dioxide Capture, Materials Science Forum. 2020;1010:367-372.

46. Antonio Blanc *et al*. Aqueous Solutions of Pyrrolidine for Carbon Dioxide Capture, Distillation Absorption, 2010, 175-180.

47. Xie HB, Zhou Y, Zhang Y, Johnson JK. Reaction mechanism of monoethanolamine with CO_2 in aqueous solution from molecular modeling. J. Phys. Chem. A. 2010;114:11844.

48. Bruder P, Lauritsen KG, Mejdell T, Svendsen HF. CO_2 capture into aqueous solutions of 3-methylaminopropylamine activated dimethyl-monoethanolamine, Chemical Engineering Science. 2012;7(5):28-37.

49. Vaidya PD, Kenig EY. CO_2-alkanolamine reaction kinetics: A review of recent studies, Chemical Engineering and Technology. 2007;30(11):1467-1474.

50. Low JJ, Benin AI, Jakubczak P, Abrahamian JF, Faheem SA, Willis RR *et al*. Virtual high throughput screening confirmed experimentally: Porous coordination polymer hydration. J. Am. Chem. Soc. 2009;131:15834.

51. Stock N, Biswas S. Synthesis of metal-organic frameworks (MOFs): Routes to various MOF topologies, morphologies, and composites, Chem. Rev. 2012;112:933.

52. Sibera D, Narkiewicz U, Kapica J, Serafin J, Michalkiewicz B, Wróbel RJ *et al*. Preparation and characterisation of carbon spheres for carbon dioxide capture, Journal of Porous Materials, 2018. https://doi.org/10.1007/s10934-018-0601-8.

53. An-Hui Lu, Guang-Ping Hao. Porous materials for carbon dioxide capture, Annu. Rep. Prog. Chem., Sect. A: Inorg. Chem. 2013;109:484-503.

54. Xing W, Liu C, Zhou Z, Zhang L, Zhou J, Zhuo S *et al*., Superior CO_2 uptake of N-doped activated carbon through hydrogen-bonding interaction. Energy Environ Sci. 2012;5:7323-7327.

55. Lu C, Bai H, Wu B, Su F, Hwang JF. Comparative study of CO_2 capture by carbon nanotubes, activated carbons, and zeolites. Energy Fuels. 2008;22:3050-3056.

56. Liu H, Cooper VR, Dai S, Jiang D. Windowed carbon nanotubes for efficient CO2 removal from natural gas. J Phys Chem Lett. 2012;3:3343-3347.

57. Przepiorski J, Skrodzewicz M, Morawski AW. High temperature ammonia treatment of activated carbon for enhancement of CO_2 adsorption. Appl Surf Sci. 2004;225:235-242.

58. Liu Y, Wilcox J. Effects of surface heterogeneity on the adsorption of CO_2 in microporous carbons. Environ Sci Technol. 2012;46:1940-1947.

59. Lu AH, Hao GP, Zhang XQ. Porous Carbons for carbondioxide capture, Green Chemistry and Sustainable Technology. 2014;2:15-77, DOI: 10.1007/978-3-642-54646-4_2,2014.

60. Serafin J, Cruz Jr. OF *et al*. Promising activated carbons derived from common oak leaves and their application in CO_2 storage, Journal of Environmental Chemical Engineering. 2022;10(3):107642.

61. Chatterjee S, Jeevanandham S *et al*. Significance of re-engineered zeolites in climate mitigation – A review for carbon capture and separation, Journal of Environmental Chemical Engineering. 2021;9(5):105957.

62. Kaye SS, Dailly A, Yaghi OM, Long JR. Impact of preparation and handling on the hydrogen storage properties of Zn_4O (1,4-benzenedicarboxylate)$_3$ (MOF-5). J. Am. Chem. Soc. 2007;129:14176.

63. Paper R. Carbon dioxide capture on metal-organic frameworks with amide-decorated pores. Nanochem. Res. 2018;3:62.

64. McDonald TM, Lee WR, Mason JA, Wiers BM, Hong CS, Long JR *et al*. Capture of carbon dioxide from air and flue gas in the alkylamine-appended metal-organic framework mmen-Mg2(dobpdc). J. Am. Chem. Soc. 2012;134:7056.

65. Valenzano L, Civalleri B, Chavan S, Palomino GT, Areán CO, Bordiga S *et al*. Computational and experimental studies on the adsorption of CO, N_2, and CO_2 on Mg-MOF-74. J. Phys. Chem. C. 2010;114:11185.

66. Claudio Pettinari, Alessia Tombesi. Metal-organic frameworks for CO_2 capture, MRS Energy and Sustainability, 2020. DOI: 10.4557/mre.2020.30.

67. Chowdhury P, Mekala S, Dreisbach F, Gumma S. Adsorption of CO, CO_2 and CH_4 on Cu-BTC and MIL-101 metal organic frameworks: Effect of open metal sites and adsorbate polarity. Microporous Mesoporous Mater. 2012;152:246.

68. Arstad B, Fjellvåg H, Kongshaug KO, Swang O, Blom R. Amine functionalised metal organic frameworks (MOFs) as adsorbents for carbondioxide, Adsorption. 2008;14:755.

69. Yazaydin AÖ, Benin AI, Faheem SA, Jakubczak P, Low JJ, Richard RW *et al*. Enhanced CO_2 adsorption in metal-organic frameworks via occupation of open-metal sites by coordinated water molecules. Chem. Mater. 2009;21:1425.

70. Reza Kazemi M, Shirazein S. Computational Simulation of Mass Transfer in Molecular Separtion Using Microporous Polymeric Membranes, Chem. Eng. Technol. 2018;41(10):1975-1981.

71. Pettinari C, Tabacaru A, Boldog I, Domasevitch KV, Galli S, Masciocchi N *et al*. Novel coordination frameworks incorporating the 4,4′-bipyrazolyl.pdf. Inorg. Chem. 2012;51:5235.

72. Vismara R, Tuci G, Mosca N, Domasevitch KV, Di Nicola C, Pettinari C *et al*. Amino-decorated bis (pyrazolate) metal-organic frameworks for carbon dioxide capture and green conversion into cycliccarbonates, Inorg. Chem. Front. 2019;6:533.

73. Hong DH, Paik M. Enhancing CO_2 separation ability of a metal–organic frameworkby post-synthetic ligand exchangewith flexible aliphatic carboxylates. Chem. Eur. J. 2014;20:426.

74. Tranchemontagne DJ, Mendoza-Cortés JL, O'Keeffe M, Yaghi OM. Secondary building units, nets and bonding in the chemistry of metal-organic frameworks. Chem. Soc. Rev. 2009;38:1257.

75. Jia T, Gu Y, Li F. Progress and potential of metal organic frameworks (MOFs) for gas storage and separation: A Review, Journal of Environmental Chemical Engineering, 2022. doi.org/10.1016/j.jece.2022.108300.

76. McDonald TM, Ram W, Lee W, Mason JA, Wiers BM, Seop Hong C *et al*. Capture of carbon dioxide from air and flue gas in the alkylamine-appended metal−organic framework mmen-Mg_2(dobpdc). J. Am. Chem. Soc. 2012;134:7056.

77. Links DA, Huang Y, Qin W, Li Z. Enhanced stabilityand CO_2 affinityof a UiO-66 type metal–organic framework decorated with dimethyl groups. Dalton Trans. 2012;41:9283.

78. Lau CH, Babarao R, Hill MR. A route to drastic increase of CO_2 uptake in Zr metal organic framework UiO. Chem. Commun. 2013;49:3634.

79. Dhakshinamoorthy A, Santiago-Portillo A, Asiri AM, Garcia H. Engineering UiO-66 metal organic framework for heterogeneous catalysis. Chem Cat Chem. 2019;11:899.

80. Marshall RJ, Forgan RS. Postsynthetic Modification of Zirconium Metal-organic Frameworks, Eur. J. Inorg. Chem. 2016;27:4310-4331.

81. Guo X, Zhu G, Li Z, Sun F, Yang Z, Qiu S. A lanthanide metal-organic framework with high thermal stability and available Lewis-acid metal sites. Chem. Commun. 2006;1:3172.

82. Devic T, Serre C. High valence 3p and Transition metal based MOFs, Chem. Soc. Rev. 2014;43(16):6097-6115.

83. Younas M, Rezakazemi M *et al*. Recent progress and remaining challenges in Post-Combustion CO_2 capture using Metal-organic Frameworks, Prog. Energy Combust. Sci. 2020;80:100849.

84. Lesch DA. Carbon Dioxide Removal from Flue gas Using Microporous Metal Organic Frameworks, UOP LLC: Des Plains, IL, 2010.

85. Planas N, Dzubak AL, Poloni R, Lin LC, McManus A, McDonald TM *et al*. The mechanism of carbon dioxide adsorption in an alkylamine-functionalized metal-organic framework. J. Am. Chem. Soc. 2013;135:7402.

86. Eli Samchez-Gomzalex *et al*. Bottleneck Effect Explained by Le Bail Refinements: Structure Transformation of Mg-CUK-1 by confining H2O Molecules, materials. 2020;13:1840-1846.

87. Guillerm V, Xu H, Albalad J, Imaz I, Maspoch D. Postsynthetic Selective Ligand Cleavage by Solid-Gas Phase Ozonolysis Fuses Micropores into Mesopores in Metal-organic Frameworks, J. Am. Chem. Soc. 2018;140(44):15022-15030.

88. Mariany Depra C *et al*. Carbondioxide capture and use in photobioreactors: The role of the carbondioxide loads in the carbon footprint, Bioresource Technology. 2020;314:123745-53.

89. Tao Wang. Carbon Dioxide Capture and Utilization-Closing the Carbon Cycle, Energy Fuels. 2019;33:1693.

90. Alessio Mezza *et al*. An Electrochemical plateform for the Carbon Dioxide Capture and Conversion to Syngas. 2021;14:7869-81.

91. Jerome MP, Alahmad FA *et al*. Layered double hydroxide (LDH) nanomaterials with engineering aspects for photocatalytic CO_2 conversion to energy efficient fuels: Fundamentals, recent advances and challenges, Journal of Environmental Chemical Engineering. 2022;10(5):108151.

92. Rehman A, Nazir G *et al*. Electrocatalytic and Photocatalytic sustainable conversion of carbon dioxide to value added chemicals: State of the art progress, challenges and future directions, Journal of Environmental Chemical Engineering. 2022;10(5):108219.

93. Godin J, Liu W *et al*. Advances in recovery and utilization of carbon dioxide: A brief review, Journal of Environmental Chemical Engineering, 2021. doi.org/10.1016/j.jece.2021.105644.

94. Li X, Wang X, Hu X, Xu C, Shao W, Wu K. Direct conversion of CO_2 to graphene via vapor-liquid reaction for magnesium matrix composites with structural and functional properties, Journal of Magnesium and Alloys, 2021. doi.org/10.1016/j.jma.2021.06.012.

Chapter 4

Biomedical and Agricultural Applications of Nanomaterials

Ferooze Ahmad Rafiqi[1]* and
Syed Kazim Moosvi[2]

Abstract Nanomaterials and their diversified applications have been the main foci of modern scientists, academicians and industrialists. Nanomaterials possess important features such as high surface to volume ratio, chemical selectivity of surface sites and show quantum effect. Owing to these features, they find applications in almost every walk of life such as electronics, health, cosmetics, sports goods, agriculture, textiles, catalysts, environment, solar cells etc. In this chapter, biomedical and agricultural applications have been discussed. Nanomaterials are used to

Ferooze Ahmad Rafiqi[1]* and Syed Kazim Moosvi[2]
[1]Department of Chemistry, Government Boys Degree College Anantnag, J&K, India
[2]School Education Department, Government of Jammu & Kashmir, J&K, India
*Email: feroozerafiqi@rediffmail.com, msyedkazim@gmail.com

cure different kinds of malignancies and neurodegenerative disorders. These materials are used to control pests and diseases, precision farming and in agronomy.

Keywords Nanomaterials, biomedical, agriculture, applications

Applications of nanomaterials in biomedical field

Nanotechnology is a new scientific approach to examine and investigate the materials in nanoscale using their physical and chemical properties [1]. It encompasses all fields of life ranging from biomedical to agriculture. It is a science of myriad of all streams that includes physics, biophysics, chemistry, biochemistry, chemical engineering and material science [2]

Applications of nanomaterials in biomedical field are numerous. In pharmaceutical field, efficacy of nanomaterials is usually determined by the nature and structure of molecules. Pharmaceutical nanotechnology is classified into two types nanostructures and

noncrystalline materials as depicted in the **Figure 1**. Nanostructure may be a nanotube (CNT), a dendrimer, a vesicle or nanoparticles [3].

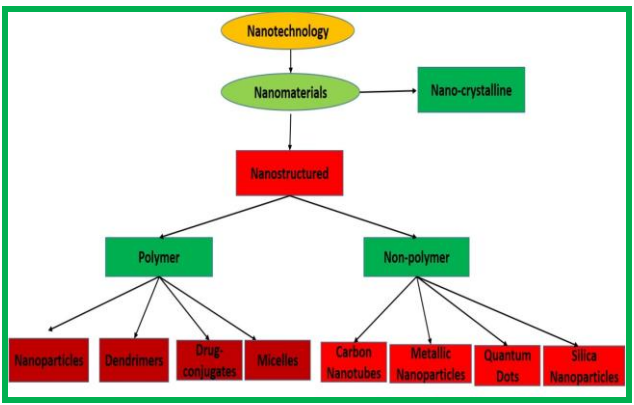

Figure 1. Schematic diagram of different types of pharmaceutical nanotechnology.

Nanotubes have distinct size, shape and have unique properties. Due to distinct shape of these nanotubes, they have some merits over the conventional drug delivery materials. Nanoparticles are extensively used as agents in drug delivery. These particles are used in the

treatment of cancer and also play a role in biosensors. Among metallic nanoparticles, silver and gold are prominent ones especially in biomedical field. Liposomes are considered to be a novel nanocarrier for drug delivery due to their small sizes. When dry lipids are put in a moisturized environment, closed vesicles are formed. Biocompatibility, versatility and entrapment efficiency are the important feature of these closed vesicles called liposomes. Dendrimer are multibranched tree-like structures (**Figure 2**). A dendrimer has a core region, a branching unit and closely packed surface. It has a globular structure and contains internal cavities. Its size is very small even less than 10 nm. These are used in controlled and targeted delivery of bioactive materials. They are efficient liver target delivery agents and cure serious hepatic ailments.

New devices like in vivo imaging and tools using nanotechnology are in constant use [4]. Some of the techniques discussed below show desired results in the early detection of a tumour cell in the body.

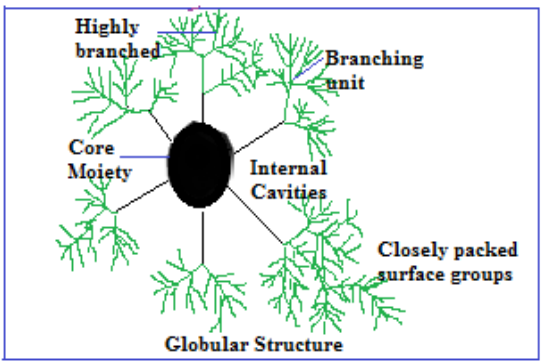

Figure 2. Schematic diagram of dendrimers depicting core branches and surface.

1. *Nanowires:* Nanosize wire or nanowire is arranged across a microfluidic channel. On passing nanoparticles through this microfluidic channel, specific molecular signatures of these particles are being coded by the sensors present on the nanowires. The information stored is then passed through a series of electrodes to the researcher. In this way, transformed genes associated with cancer are detected.

2. *Cantilevers:* These are beams carrying molecules capable of ligating specific substrates. Such devices detect even a single molecule of DNA or a protein. Cancer cells secrete proteincious products. The antibodies present on the cantilever selectively bind with the secreted proteins. These antibodies are fabricated in a way so as to pick up a single or more distinctive molecular expression of a malignant cell. At the event of binding, there has been observed a change in the conductance of the cantilever, thus aiding in detecting related molecules in a rapid and sensitive way.

3. *Nanoparticles:* These are target oriented. Radiolabelled nanoparticles have been used in the past to detect a tumour malignant cell. They are safely injected into the body. They bind favourably to the cancer cell making it visible. Through conventional imaging, it was very difficult to visualize a tumour cell. This problem has now been solved after the discovery of these nanoparticles. Whether a cancer cell is badly

injured or is actually stimulated, it was difficult to diagnose. This problem is again solved by using nanoparticles as visualizers. Nanoparticles may be a biological entity or a chemical moiety. Biologically, a nanoparticle may be a lipid, phospholipids, lactic acid, dextran, or chitosan and chemically, it may be a metal, polymer, silica, carbon etc.

4. *Carbon Nanotubes:* They help in diagnosis of the disease by identifying the exact location of the DNA molecule. Bulky molecules are tagged with mutated areas linked with cancer. Using the nanotube tip, physical shape of DNA is traced. This information is digitally translated into a topographical map. Thus, the exact location of the mutated area is easily pinpointed on the map with the help of the tagged bulky molecules.

5. *Quantum Dots:* When these crystals are exposed to UV light, they glow and emit colour that depends on their size. These crystals are impregnated to a molecule that binds with the substance of interest and

glow at the event of binding. Due to various colours emitted by the quantum dots, several substances can be detected simultaneously e.g multiple proteins are detected by imaging with the help of fluorescent quantum dots.

Nanotechnology in medicine

Medicine synthesized in the nanoscale is called nanomedicine. Nanomedicine is target oriented. It identifies a defect or a disease in the body at the earliest stage. It works on the principle of detection of a single defective cell and then curing or treating it. The nanoparticles due to their small size find way in the oncology field, particularly in imaging. Quantum dots are the nanoscale particles having quantum confinement properties such as size-tuneable light emission. Such a property can be used in conjugation with magnetic resonance imaging (MRI), to display exceptional images of tumor sites. Nanoparticles when compared to organic dyes require one light source for excitation and emissions are much brighter. Using fluorescent

quantum dots, a higher contrast image that too at a lower cost is produced as compared to conventional organic dyes. The new nanomaterials used have good efficacy in function like diagnosing, preventing and treating cancers. The methods are being developed for early detection and molecular imaging of cancer. Nanowires, nanotubes and cantilevers detect the cancer biomarkers timely and efficiently. Metastatic lesions in lymph nodes are precisely spotted by using nano sized iron oxide particles coupled with MRI.

Nanotechnology in Drug Delivery

Drug delivery is one of the prioritized objectives of nanomedicine research by using nanotechnology. Improvement of pharmokinetic and pharmodynamic properties of the drug is achieved by using nanoscale particles or molecules. Nanotechnology and the techniques involved in it has successfully overcome the poor bioavailability of drugs. Bioavailability is considered to be an important factor in evaluating the pharmokinetic properties of a drug. An exchequer of about 65

billion dollar is wasted every year because of the poor bioavailability of the drugs. Keeping this aspect under consideration, novel way of drug synthesis is required. Drug delivery has been significantly improved by the usage of nanoscale drugs. Nanoparticles being very small in size unlike other bigger elements are taken up by the cells in an easy and trouble less way. Using nanoparticles, prolonged and targeted action of the drug has been augmented besides reducing the drug dose. The main goal of nanotechnology is to increase bioavailability. Sometimes it has been observed that the drug activity has decreased while increasing bioavailability as has been observed in case of insulin chitosan nanoparticle. Due to the small size of nanoparticles, there is reduction in the particle size of the partially soluble drugs, thus resolving the drug insolubility problem. By using nano-drugs, there has been an improvement in the dissolution of the drug and bioavailability besides reduces the toxicity and dozing level of the drug [4]. A dendrimer provides a tailored sanctuary for the drugs as it contains various voids. The voids provide ample space for the

drug molecules and the structure protects them from the outside environment. In this way, the drug molecules are trapped and the drug is safely released at the tumour site.

Micelles (**Figure 3**) are aggregates of amphiphatic molecules having a hydrophilic polar end and a lipophilic hydrocarbon tail. Polar ends are oriented outwards forming the exterior surface and non-polar end towards the interior forming the core. Drugs which are hydrophilic can be safely stored in the core of micelles shields the drug from the external environment. Drugs which are hydrophilic are preferably adsorbed at the miceller surface. If the drug is amphiphatic, the molecules may adjust themselves in a particular alignment.

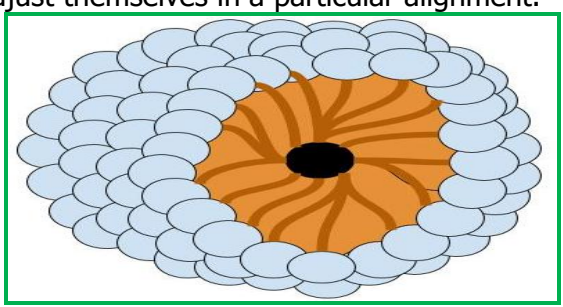

Figure 3. Micelle Molecule.

Treatment of Vascular Thrombosis

Nanoparticles are used as carriers for thrombolytic drugs. Thrombolytic drugs cure Vascular Thrombosis. Thrombosis is the formation of blood clots. Thrombolytic drugs when administered to a patient systematically may result in hemorrhage. Orally such drugs are less effective. Such drugs after incorporation into nanocarriers increase their efficacy of action. They are released directly into the specific site and side effects produced are reduced to minimal [4].

Gene Therapy

Nanoparticles are used as carriers for gene therapy, for example, plasmid DNA is engulfed in PEG-modified gelatin nanoparticles. Both single and double stranded DNA as well as RNA are transported by dendrimers. Solid lipid nanoparticles and closed vesicles like liposomes are used as carriers for gene transfer.

Hepatic Targeting

Nanoparticles are engulfed by the phagocytic system of the spleen and liver. Liver diseases like hepatitis and tumor metastasis are treated efficiently by this technique of hepatic targeting using these nanoparticles [5]. Kidney diseases are treated in the same way. Nanomedicines and nano-imaging process helps to study cellular process in kidney cells.

Treatment of Neurodegenerative Disorders

One more application of nanotechnology is the treatment of neurodegenerative disorders [6]. Nanocarriers such as nanogels, polymeric nanoparticles, liposomes, dendrimers and nanoemulsions are used in the drug delivery of CNS therapeutics.

Nanotechnology in Agriculture

Nanotechnology played a vital role in revolutionizing the agriculture sector. New

tools and approaches have been developed at the molecular level to study the origin and treatment of diseases. Nanotechnology helps to know the mechanism of rapid detection of diseases and the ability of crops to take nutrients beyond their normal capacity. To combat viruses and other crop pathogens, smart delivery system and smart sensors have been devised in the agricultural industry. In the near future scientists are planning to come up with new innovative nanostructured catalysts. Such type of catalysts may increase the efficiency of pesticides, thereby reducing the dose level required. Nanoparticles have higher solubility in suspension. Because of this property, nanomaterials easily penetrate seed coats and emerging roots and provide bioavailability of molecules to the seed radicals [7]. Nanomaterials have improved targeted activity [8] and provide actual concentration and controlled release of fertilizers and pesticides [2] besides lowers negative environmental concern of pesticides. TiO_2 nanoparticles act as fertilizer carrier for Mug bean plant and increase the crop yield significantly [9].

Precision Farming

It has been a dream of agriculturalists to have maximum output (crop yield) and minimum input (pesticides and fertilizers). This can be achieved only through the mechanism of accurating target action and monitoring environmental variables. The important role that the nanotechnology enabled devices is to link autonomous sensors with a global positioning system for real time monitoring. These nanosensors are distributed in the field so as to monitor the crop growth and soil conditions. The biotechnology and nanotechnology should work in synergy to create equipments of augmented sensitivity, thereby responding to environmental changes quickly. Due to the small size of CNTs and nanocantilever sensors, individual proteins or molecules are trapped and measured accurately. Nanoparticles are engineered to stimulate an electric or chemical signal. Nanosensors can work also by an enzymatic action. Dendrites are used as probes to find a particular chemical moiety such as a protein. Eventually precision farming using small

sensors can enhance productivity in agriculture by providing exact data and accurate information, thus assisting farmers to speculate better decisions [10].

Agronomy

Agronomy is the science of soil management and crop production. As discussed already, precision farming is a new practice in farm management. Nanosensors have added beauty and flavour to farm management. By this method, one is able to assess how much fertilizers are required per patch of the farm and help the farmers to maintain his farm with precision control. Therefore, the aim of using minimum output and maximum output such as safe products can be easily achieved. Use of nanosensors and nano-based delivery system will increase the efficiency in the use of agricultural resources like nutrients, chemicals and water through precision farming. Linking nanomaterials and global positioning system with satellite imaging of the field can detect a crop pest or a drought condition remotely. Once a pest or a drought is detected in the

field, it is immediately combated with the application of pesticides or adequate irrigation level. Soil nutrient level and presence of any plant virus in the field can be detected by using nanosensors. Nanofertilizers are absorbed by plants rapidly and efficiently. There is a new trend of saving fertilizers and reducing environmental pollution by using nano-encapsulated slow release fertilizers. Slow release fertilizers are considered as excellent substitutes to soluble fertilizers. Using slow release fertilizers, nutrients are taken up by the plants without any waste as the nutrients are released at a slower rate. Otherwise the nutrients are wasted by leaching. Another class of materials called zeolites which are naturally occurring minerals having a honey comb like structure. Zeolites have a network of cage like structures. The cages of zeolites are loaded with nitrogen and potassium along with other ingredients (phosphorus, calcium and trace nutrients). After coating and cementing nano and sub-nano composites, they are capable of releasing the nutrients from the fertilizer capsule in a controlled manner [11].

Nanotechnology also finds application in agricultural machinery such as manufacturing and designing machine parts and agricultural tools. Coating of nanotube over the mechanical parts of a machine makes it light and strong. A strong mechanical component of a machine retard the corrosion lessens the UV rays effect and resists against the wear and tear. Smart machines using biosensors are used for mechanical-chemical weed control. Friction is reduced by nanocovering over bearings. Nanotechnology has shown its ability to modify the genetic constitution of the crop plants thereby improving the crop plant variety [12, 13]. Smart seed is prepared when a seed is imbibed with nano-encapsulated particles loaded with bacterial strain. Smart seed can reduce seed rate and improves crop performance. A smart seed is programmed and germinates only when adequate moisture is available. The spray can be sprinkled to the seed over a mountain range for reforestation. Nano-SiO_2 is used to enhance the characteristics of tomato seed germination [14].

Pests and plant disease management

Insecticides, fungicides and herbicides have been used since several decades in controlling pests and plant diseases. No doubt, it is the cheapest and fastest way to control pests and diseases but unprecedented use of them have adverse effect on human health, pollinating insects and domestic animals. Such contaminants after entering into the ecosystem have become an alarming curse. Availability of pesticides in the nanoparticle or nanocapsule form has the desired and efficient results. These nanoscale particles are environmentally benign, effective in action and yield better results in lower dose. There are countless nanomaterials that include polymeric nanoparticles, Fe_2O_3 nanoparticles, Au nanoparticles which can be easily synthesized and exploited as pesticide or drug delivery piggybanks [15].

Conclusion

Nanomaterials are used as nanomedicines, drug delivery carriers and have

agricultural applications. Nanomedicine is used to cure cancer, gene therapy and other dreadful diseases. Nanoscale materials act as carriers for drugs and treats diseases like vascular thrombosis, liver and kidney ailments and neurodegenerative disorders. Nanomaterials are used for the better soil management, rapid disease detection in plants, pest control and improve the production of crops. Nanoparticles can deliver active ingredients or drug molecules to any part of the plant to end pathological sufferings.

References

[1] W.F. Abobatta, Nanotechnology application in agriculture. Acta Scientific Agriculture, 2018, 2:99-102

[2] S.H. Abd-Elrahman, M.A. Mostafa. Applications of nanotechnology in agriculture: an overview. Egyptian Journal of Soil Science, 2015, 55:197-214.

[3] A.P. Nikalje. Nanotechnology and its applications in medicine. Medicinal chemistry, 2015, 5:081-089.

[4] Y. Pathak, D. Thassu, M. Deleers.

Pharmaceutical Applications of Nanoparticulate Drug-Delivery Systems. Nanoparticulate drug delivery systems, 2007, 166-185.

[5] W.H. De Jong, P.J. Borm. Drug delivery and nanoparticles: applications and hazards. International journal of nanomedicine, 2008, 3:133-149

[6] H.L. Wong, X.Y. Wu, R. Bendayan. Nanotechnological advances for the delivery of CNS therapeutics. Advanced drug delivery reviews, 2012, 64:686-700.

[7] C.A. Dehner, L. Barton, P.A. Maurice, J.L. DuBois. Size-dependent bioavailability of hematite (α-Fe2O3) nanoparticles to a common aerobic bacterium. Environmental science & technology, 2011, 45:977-983.

[8] C. Lu, C. Zhang, J. Wen, G. Wu, M. Tao. Research of the effect of nanometer materials on germination and growth enhancement of Glycine max and its mechanism. Soybean Science, 2002, 21:168-171.

[9] R. Raliya, P. Biswas, J.C. Tarafdar. TiO2 nanoparticle biosynthesis and its

physiological effect on mung bean (Vigna radiata L.). Biotechnology Reports, 2015, 5: 22-26.

[10] J. Tiju, M. Morrison. A nanoforum report. Nanotechnology in Agriculture and Food. Institute of Nanotechnology, European nanotechnology Gateway, 2006:1-14

[11] X.M. Liu, Z.B. Feng, F.D. Zhang, S.Q. Zhang, X.S. He. Preparation and testing of cementing and coating nano-subnanocomposites of slow/controlled-release fertilizer. Agricultural Sciences in China, 2006, 5:700-706.

[12] Y. Shang, M. Hasan, G. J. Ahammed, M. Li, H. Yin, J. Zhou. Applications of nanotechnology in plant growth and crop protection: a review. Molecules, 2019, 24(14), p.2558.

[13] M.C DeRosa, C. Monreal, M. Schnitzer, R. Walsh, Y. Sultan. Nanotechnology in fertilizers. Nature nanotechnology, 2010, 5:91.

[14] M.H. Siddiqui, M.H. Al-Whaibi. Role of nano-SiO2 in germination of tomato (Lycopersicum esculentum seeds Mill.). Saudi journal of biological sciences,

2014, 21:13-17.

[15] M. Sharon, A. K. Choudhary, R. Kumar. Nanotechnology in agricultural diseases and food safety. Journal of Phytology, 2010, 2: 83–92.

Available online at www.elixirpublishers.com (Elixir International Journal)

Applied Chemistry

Elixir Applied Chemistry 178A (2023) 56855 - 56867

ISSN: 2229-712X

Removal of Methylene Blue Dye from Aqueous Solution on to Novel Adsorbents: Molybdenum Dicarbonate-Filter Paper and Molybdenum Dicarbonate-Activated Carbon Composites

Ferooze Ahmad Rafiqi*, Shabir Ahmed Bhat and Raveed Yousuf Bhat
Govt. Degree College Anantnag, Department of Higher Education, Jammu and Kashmir, India.

ARTICLE INFO

Article history:
Received: 15 March 2023;
Received in revised form:
1 May 2023;
Accepted: 10 May 2023;

Keywords
Molybdenum Dicarbonate;
Filter Paper;
Activated Carbon;
Adsorption;
Wastewater Treatment.

ABSTRACT

Two composites-1) Molybdenum dicarbonate-filter paper and 2) Molybdenum dicarbonate-activated carbon were synthesized and characterized by X-ray diffraction (XRD), scanning electron microscopy (SEM) and energy dispersive X-ray analysis EDX. Using the method of UV-visible spectroscopy, the removal efficiences and adsorption capacities of these composites towards the removal of methylene blue (MB) from aqueous solution were compared. The findings of the MB adsorption with these composites (I and II) indicated equilibrium adsorption in less than 5 minutes. Composites I and II have MB removal efficiencies of 87% and 96.25%, respectively, and their estimated adsorption capacities at 20°C are 432 mg g^{-1} and 481 mg g^{-1}. The adsorption process of MB onto Molybdenum dicarbonate-filter paper (composite I) suited well with the pseudo-first order and pseudo-second order kinetics and conformed to intraparticle diffusion model for Molybdenum dicarbonate-activated carbon composite (composite II). Adsorption of MB onto composite I aligned with both Freundlich model and Tempkin models due to higher values of correlation coefficients and fitted well with Langmiur model for composite II. Adsorption process was found to be endothermic and spontaneous in nature. The adsorption results revealed that these composites could be employed as effective adsorbents to remove dyes from industrial effluents.

1. Introduction

Freshwater fit for drinking on earth is less than 1.5 pecent of the total earth's 3 percent freshwater quantity[1]. To cater the water requirements of 8 billion people with this meagre amount of drinking water is undoubtedly a great challenge for this century. This problem has been further exacerbated due to the impacts of climate change. The manufacturing industries especially the textile industies consume unmeasurable quantity of water that generates tonnes of effluents which require advanced technologies for treatment and purification[2].

Dyes and pigments used in textile industry are water-intensive as very large amount of water is consumed during the dyeing of fabrics. At an average, 10^7 Kg of dyes are consumed per year out of which 10^6 are discharged into waste streams alone by textile industry [3]. One Kg of textile requires 200L of water at an estimated approximation. This dyeing of textiles thus further adds the existing deteriorated drinking water scenario of the world.

More than 10.000 dyes and pigments are used worldwide out of which methylene blue (MB) is amongst the most commonly used dye[4]. In this work, we have picked Methylene blue (MB) dye and investigated it as a test probe for remedial experiments. Methylene blue is mainly used as a dye in textile, printing, food industries and distilleries[5], besides being employed as a chemical indicator and ISO test pollutant in semiconductor photocatalysis[6]. Although this dye has some medicinal and pharmaceutical applications [7, 8] but its release in water bodies poses threat not to aquatic ecosystem but to human beings too[9]. MB molecule has an aromatic structure thus rendering it poor biodegradibility. This dye imparts color to the surface water thus reduces the penetration of sunlight depriving the algae to undergo normal photosynthesis. This dye increases the chemical oxygen demand in the water besides triggering bioaccumulation in human food chain [10-12]. MB engenders different diseases in human beings like gastrointestinal tract infection, dermatitis, Heinz body formation, quadriplegia, jaundice, allergy and can stimulate mutations in human beings [13-15], thus it has serious environmental concerns. It is now essential for industrialists, chemists, and environmentalists to decontaminate it in wastewater streams and reduce its utilisation in industry in order to accomplish sustainable water management and to preserve a healthy and environment-friendly life structure on earth. Various chemical, physical and biological methods were used worldwide in scavenging the dyes and pigments, heavy metals and other toxins from industrial effulents and other real water samples and sources. These methods include membrane filtration, reverse osmosis, flocculation, sedimentation, liquid-liquid extraction, dialysis, biological oxidation and adsorption[16-20]. Among the listed methods, adsorption is the most efficient and reliable physicochemical treatment method of heavy metal and dye-bearing wastewater[21-23]. This is because of good ecnomics, simple procedure, simplicity of design, environment-friendly and efficient method amongst the all methods available.

Tele: +919797237588
E-mail address: feroozerafiqi@rediffmail.com

Adsorbents based on agricultural waste that are non-conventional and renewable sources have received considerable attention in dye-bearing wastewater treatment from last few decades. The use of bioresource as adsorbents is still in vogue and are demanded by the research community globally because of their low cost, abundance, easily available, high adsorption capacity than conventional adsorbents and high selectivity towards toxins [24-26].

As per the research findings over the use of biowaste material as adsorbents are concerned, some prominent examples are pine-fruit shell, spent coffee, tree fern, palm oil mill effluent waste, orange peel, rice husk, orange peel, wheet shells, corn husk, bamboo dust, sugar beet pulp, spent tea leaves, seeds, Shorea roxburghii, saw dust and catha edulas stem[5,6,9,11-14, 16]. Almost every part of the plant/tree has been tested as adsorbent and have proven as efficient materials for waste water treatment [27-31]. These agricultural wastes and other bioresource materials are used with slight or heavy physical and chemical modifications. These changes include carbonation, acid-alkali hydrolysis, bleaching and extracting methods, drying, ultrasoication, heating under different condition and various physical processes [4-6, 9-13]. The fundamental components produced by diverse physical and chemical processes on agricultural and forestry products are cellulose and activated carbon. After processing, these materials are made accessible for commercial sale. Powdered activated charcoal and filter paper are two examples.

In this study, the cellulose chains of filter paper were doped with molybdenum dicarbonate (MoC_2O_6), and the activated carbon was likewise blended with the same complex. Applications for molybdenum complexes are numerous in research and technology [32–34]. The uncoordinated lone pairs on the two oxygen atoms in this complex can impart a basic character in them, which is the major reason for employing it as a component in the composite formation. These composites are good candidates for use as adsorbents in the wastewater treatment process for the removal of cationic dyes like MB due to their basic nature. The efficiency removal percentage of these prepared composites are much higher than various reported results. This is supported by the fact that employing these new composites, 96.25% and 87% of MB are removed from an aqueous solution within 5 minutes at 20°C.

The principal objectives of this study are: (1) successful synthesis of Molybdenum dicarbonate (MoC_2O_6)-filter paper composite and MoC_2O_6 modified activated carbon, (2) Use of these composites as adsorbents towards the removal of MB from aqueous solutions and to examine their adsorption capacities, (3) To investigate the effects of contact time, dosage, pH, temperature and concentration of MB on the adsorption behaviour, and (4) to evaluate different kinetic and thermodynatic parameters.

2. Experimental

2.1. Materials

Ammoium molybdate {$(NH_4)_2MoO_4$} of Merck quality and methylene blue (MB) of Qualigens chemicals were used. Whatman filter paper and powdered activated charcoal were purchased from Loba chemicals and utilised exactly as received from the supplier. MB has the chemical formula $C_{16}H_{18}N_3SCl$. It dissolves in water at a rate of 43.2 g/L at 20 °C, and when MB is dissolved in water, a blue cationic dye is generated. In its cannonical structure, it has a positive charge either on nitrogen or sulphur. Sodium Carbonate, ethanol and ammonia were also supplied by Loba chemicals. In the synthesis and experimentation part, doubly distilled water was used.

2.2. Instrument and measurements

The Kipps apparatus was used for the production of hydrogen sulphide gas. XRD data was obtained using PW 3050 base diffractometer with CuK_α radiation of 1.540598 Å. Surface morphology of the samples were carried out on ZEISS EVO series scanning electron microscope model EVO50. The textural properties were determined by N_2 adsorption desorption at 75 K using an ASAP 2420 system by Brunaur-Emmet-Teller method. Energy dispersive X-ray (EDX) of Bruker model was resorted to investigate the elemental composition of molybdenum complex and its successful insertion into the synthesized composites. In order to determine the maximum wavelength of MB, equilibrium concentration and adsorption kinetics, Ultravoilet-visible (UV-vis) spectra were taken on double beam UV-Visible spectrophotometer T 80. This spectrophotometer has a scan range of 200-1100 nm wavelength and a cell of 1cm optical path length.

2.3. Synthesis

2.3.1. Synthesis of Molybdenum dicarbonate (MoC_2O_6)

Using a magnetic stirrer, 49 grams of the salt is dissolved in 250 ml of distilled water to create a 1 M ammonium molybdate solution. In the presence of 10 ml of ammonia, the hydrogen gas generated by the Kipps device is passed through this molybdate solution. This mixed solution is added a 1 M sodium carbonate solution. The entire solution has been heated at 60°C for 30 minutes. Crystals of a dark crimson colour are precipitated. The solution is filtered and repeatedly rinsed with ethanol after standing for 24 hours. The sample is dessicated for 48 hours after being dried in an oven at 90 °C. A little portion of the synthesis was completed using well-established synthesis techniques [35].The following reactions are expected to occur in the aqueous media in the presence of ammonia.

StepI: $(NH_4)_2MoO_4 + 4H_2S \xrightarrow{aqueous\ ammonia} (NH_4)_2MoS_4 + 4H_2O$

Step II: $(NH_4)_2MoS_4 + 2Na_2CO_3 \xrightarrow{\Delta} MoC_2O_6(\downarrow) + 2\ Na_2S$

$+ (NH_4)_2S + S^{2-}\ \ S^{2-} + H_2O \longrightarrow HS^- + OH^-$

2.3.2. Synthesis of Molybdenum dicarbonate (MoC_2O_6)-filter paper Composite:

The Whatman filter papers were cut into pieces that were 1 mm in size. 1g of these cut pieces are then added to the mixture solution during the step II of the procedure of Molybdenum dicarbonate synthesis. After standing in the solution for 24 hours, it is filtered. The sample obtained during filteration is cleaned with ethanol, then dried in an oven at 50 °C, followed by 48 hours of desiccation. The reaction is schematically shown as:

$(NH_4)_2MoS_4 + 2Na_2CO_3 + \text{Filter Paper} \xrightarrow{\Delta} MoC_2O_6$-filter paper composite $(\downarrow) + 2\ Na_2S + (NH_4)_2S + S^{2-}$

2.3.3. Synthesis of Molybdenum dicarbonate (MoC_2O_6)-activated carbon Composite:

In this composite formation, 1g of activated carbon is added to the mixture solution during the step II of the synthesis of Molybdenum dicarbonate. The same procedure has been adopted for the separation of sample as adopted for composite I. The reaction is schematically shown as:

$(NH_4)_2MoS_4 + 2Na_2CO_3 + \text{activated carbon} \xrightarrow{\Delta} MoC_2O_6$-activated carbon composite $(\downarrow) + 2\ Na_2S + (NH_4)_2S + S^{2-}$

2.4. Adsorption experiments

In the adsorption experiments, the following procedure was adopted. 50 mg of MB was added to 100 ml of doubly distilled water and 10 ml of this stock solution was then treated with 100 mg of MoC_2O_6-filter paper composite

(composite I) and MoC_2O_6-activated carbon composite (composite II), separately. The solutions were manually agitated for a short span of time (1 minute). Then simple decantation process was used for the removal of adsorbent and the decant was examined for the unadsorbed MB, spectrophotometrically using the double beam spectrophotometer. Absorption spectra of MB were taken after every one minute time interval. Concentrations of MB was calculated using the equation of Lambert-Beer's Law:

$$A = \varepsilon bc \quad (1)$$

Where A, b and c are the absorbance, thickness of the cell and concentration of the MB in the solution, respectively. ε is molar extinction coefficient which is constant for a particular species at a particular temperature.

3. Results and discussion

3.1. SEM-EDS Characterization

Fig.1. (a-c) shows the SEM images of Molybdenum dicarbonate (MoC2O6), Molybdenum dicarbonate (MoC2O6)-filter paper (composite I) and Molybdenum dicarbonate (MoC2O6)-activated carbon (Composite II), respectively. SEM image of Molybdenum dicarbonate mostly shows rectangular mass of crystals indicating the agglomeration of molybdenum dicarbonate molecules. The SEM images of composites show the presence of molybdenum dicarbonate crystals on the surfaces of filter paper and activated carbon in the composites. Activated carbon shows the honey comb like structure within pores of which Molybdenum dicarbonate crystals are visible. The interaction between the components looks superficial that indicates the van der waal's type of interaction between them. The composite formation is further substantiated with the EDS spectrum that shows prominent peaks of molybdenum, carbon and oxygen as shown in Fig.2. (a-c). Weight percentage of Mo, C and O present in the Molybdenum dicarbonate are 45%, 12.20%, 20.92%, respectively. The composite with filter paper shows weight percentage of Mo, C and O 28.19%, 28.7% and 38.73%, respectively. The composite of Molybdenum dicarbonate with activated carbon shows weight percentage of Mo, C and O 33.72%, 53.19 %, and 10.82 %, respectively.

The textural properties viz. specific surface area and average pore diameter size of both the composites were calculated via BET method. Surface area of composite I is found to be 64 m2/g while as this value for composite II is 1654 m2/g. This indicates that the powdered charcoal has almost 26 times more surface area than that of filter paper in unit mass of their substances. The average pore diameter of composite I is 3.0-5.0 nmwhile as this value ranges 2.5-4.0 nm for composite II.

3.2. XRD Characterization

X-ray diffraction (XRD) analysis were carried out on PW-3050 base diffractometer with Cu Kα radiations in the scanning range of 0°-80°. Fig.3. (a-c) shows the XRD diffraction pattern of (a) Molybdenum dicarbonate (dopant), (b) Molybdenum dicarbonate-filter paper and (c) Molybdenum dicarbonate-activated carbon composite, respectively. The XRD patterns of the dopant and the composites confirms the crystallinity of the samples. The Molybdenum dicarbonate-Whatman filter paper exhibits semicrystalline peaks at 16.47 and 22.5, which are the characteristics peaks shown by cellulose structure of paper [36]. Besides these chracteristic peaks, peaks at 2θ values of 11.47, 27.20, 34.33 and 46.83 are observed in the XRD pattern of this composite which is likely because of the metal complex component of the composite. Two wide peaks at 25.04° and 43.98° are the prominent amorphous peaks of activated carbon. In the XRD pattern of the composite of activated carbon, some sharp peaks at 2θ values of 17.91, 27.20, and 33.62 have been observed which is due to the molybdenum dicarbonate component. Sharp peaks are the characteristics of crystalline substances [22], the appearance of such type of peaks in both the methyl dicarbonate and composite proves the crystalline nature of the composites. The peaks of methyl dicarbonate are appearing in both the composites with appreciable shifts that supports a good interaction between the components and confirms the successful synthesis of composites of methyl dicarbonate with whatman filter paper and activated carbon.

3.3. Efficiency removal

The following equation is generally employed to determine the percentage removal efficiency of adsorbents (composite I and II) towards the removal of dyes (MB) and heavy metals:

$$\eta=(C\_i-C\_t)/C\_i \times 100 \quad (2)$$

Where Ci and Ct are the initial concentration of MB and its concentration at time't', respectively. The concentration terms are expressed in $mgL^{-1.}$

The following equation has been used to determine the maximum adsorption capacity of the adsorbents (composite I and II) :

$$Q_e = \left(\frac{C_i - C_e}{M}\right)V \quad (3)$$

Where C_i and C_t are the initial concentration of MB and its concentration at time t', V is the volume of solution (L), and M is the mass of adsorbent (g), Q_e is maximum adsorption capacity of the adsorbent, expressed in mg/g.

3.3.1. Effect of contact time

Absorption spectra of Methylene blue adsorption by (a) Molybdenum dicarbonate (b) Molybdenum dicarbonate-filter paper and (c) Molybdenum dicarbonate-activated carbon composite, respectively. are shown in Fig.4. Absorbance of MB solutions is measured by UV-visible spectrophotometer. MB in aqueous solution exhibits maximum absorbance at 662 nm. Concentration of MB in the given aqueous solution decreases upon addition of the adsorbents. MB is removed from aqueous solutions probably through electrostatic interactions as the MB is cationic in nature. Porous nature of filter paper and activated carbon could augment the adsorption of MB.

Molybdenum dicarbonate-filter paper and Molybdenum dicarbonate-activated carbon composite have shown excellent adsorption capacities due to the synergy of Molybdenum dicarbonate and basic matrices of filter paper and activated carbon. Molybdenum dicarbonate-activated carbon composite is better adsorbent than Molybdenum dicarbonate-filter paper that is probably due to the high specific area of the activated carbon. Adsorption of 96.25% MB on the composite II and 87% on the composite I occurs within 5 minutes duration at room temperature. The adsorption efficiency removals of these composites were determined as per equation (2). However, a slight increase in the adsorption of MB onto composite I and II occurs on increasing the contact time from 5 minutes to 60 minutes. The maximum adsorption capacity of composite I and II are calculated using the equation (3) and the values are 432 mg g-1 against composite I and 481 mg g-1 against composite II. These adsorbents are excellent candidates for potential industrial applications due to their high adsorption capacities. The results are summarised in Table 1 and show that these composites have greater adsorption capabilities than activated carbon and unmodified filter paper. These higher values of composites than the neat matrices vindicate the role of molybdenum dicarbonate in

improving the sequestration potential of these prepared composites towards the MB removal. However, unmodified activated carbon shows better removal efficiency than the neat filter paper on account of its high specific area. The order of adsorption capacities follow the order: Molybdenum dicarbonate-activated carbon composite, Molybdenum dicarbonate-filter paper, Molybdenum dicarbonate complex.

The maximum adsorption capacities for MB by these adsorbents are either higher than some research findings or competetive to among the best adsorbents reported so far. The data reported in the literature is shown in Table 2. [37-46, 2,4, 6,9,10,13,15,21,23]. Molybdenum dicarbonate-filter paper and Molybdenum dicarbonate-activated carbon composite having oxygen atoms with uncoordinated lone pair of electrons can easily bind MB through electrostatic interaction. These oxygen atoms may belong either to Molybdenum dicarbonate component or the –OH function group of cellulose chains of filter paper. Further the MB molecules can be entrapped within the micro and mesopores of the composites [24-31]. The mechanism of adsorption of MB on composite I and II involves more than one type of interactions. However, electrostatic attraction between oppositely charged sites plays a dominating rule in the adsorption of MB. Molybdenum dicarbonate with uncoordinated lone pair of electrons on oxygen atoms makes the composite I and II an exclusively electron rich substrates where cationic dyes like MB can be easily lured and bound. This property makes thes composites an ideal candidate for cationic dye removal in real wastewater samples. The hydroxyl and oxygen units of cellulosic part of paper also enhances the adsorption capacities towards the cation dye MB molecules.

3.3.2.Effect of initial concentration of MB dye

About 87% and 96.25% of the adsorption of MB onto composite I and composite II occurs within 5 min. This can be both because of the (i) electrostatic attraction between the cationic MB dye molecule and oxygen atoms of methyl dicarbonate (ii) Interaction between MB with hydroxyl groups of filter paper and (ii) also due to trapping of MB molecules within pores of the composites. With the increase in the concentration of MB, the adsorption gradually decreases. This may either be because of the full occupancy of active sites or the agglomeration of MB dye molecules. Aggregated MB molecules further can dissuade the individual free molecules to move deeper inside the porous core of the composite. Under the same initial dye concentration, the adsorption capacity of composite II is better to that of composite I as shown in Table 3. This may be because of the large specific surface area and higher porous density of composite II.

3.3.3. Effect of pH

The adsorption of MB onto the composite I and composite II varies with the pH of the solution. Both composite I and composite II show excellent adsorption at pH 7 and less adsorption in alkaline solution and least in acidic solution. At low pH, uncoordinated oxygen atoms of molybdenum dicarbonate and hydroxyl of cellulosic part of filter paper are highly protonated, thus, develops a positive charge throughout the adsorbent, therefore, shows low adsorption affinity towards MB elimination from the conc. HCl solution. At higher pH, OH-ions affects the free motion of cationic MB molecule because of electrostatic neutralization, thereby makes their attraction a bit low towards the active sites of adsorbents. The results obtained are summarized in Table 4. The order of removal of MB by the adsorbents follows the order: Neutral medium, alkaline medium, acidic medium.

3.3.4. Effect of adsorbent dosage

Fixed quantity of MB aqueous solution (10 ml of 50 mg L-1 MB) is treated separately with adsorbents (composite I and II) in the quantity ranging from100-500 mg in the increments of 100 mg. Adsorption of MB onto these composites are then investigated at each dose of adsorbent. The removal percentage of MB from aqueous solution increases with the increase in the amount of adsorbent dose. It is mainly because of the increase in the number of active sites, surface area and also because of increase in pore number of adsorbents. Molybdenum dicarbonate having uncoordinated oxygen atoms provides biding sites to positively charged MB molecule. The removal efficiency is higher for composite II as compared to Composite I at all adsorbent dose levels that might be because of large surface area of the composite II.

3.3.5. Effect of Temperature

50 mg of MB was dissolved in 1L of doubly distilled water. 10 ml of this stock solution was treated separately with 100 mg of composite I and II for a contact time of 5 minutes at 20°C. It was then decanted and the decant part was examined by UV-visible spectroscopy. Stock solution was heated to 40°C, 60°C, 80°C and 100°C and at each temperature, the above procedure was adopted (10 ml of stock solution treated with 100 mg adsorbent). Adsorption of MB onto both composites continuously increased from 20°C to 80°C due to the enhanced thermal motion of MB particles in the aqueous solution and the adsorption capacities at different temperatures are shown in Table 5. At 100°C, adsorption starts decreasing to a little extent indicating the commencement of desorption phenomenon of MB molecules.

3.4. Adsorption kinetics

The following pseudo-first-order equation which is also known as Lagergren first order rate equation is based on concentration of the solution and adsorption capacity of the solid:

$$\text{Log } (Q_e\text{-}Q_t) = \log Q_e - \frac{K_1}{2.303} t \quad (4)$$

The following pseudo-second-order rate expression is also based on the adsorption capacity of solids:

$$\frac{t}{Q_t} = \frac{1}{K_2 Q_e^2} + \frac{t}{Q_e} \quad (5)$$

The intra-particle diffusion model described by Weber and Morris is based on the concentration of adsorbate 'C' expressed in mg L-1 and is represented by the following equation:

$$Qt = kit1/2 + C \quad (6)$$

Where k_1, k_2 and ki are rate constants for pseudo-first-order, pseudo-second order and intra-particle diffusion models, respectively. Q_e and Q_t represents the adsorption capacity (amount of MB adsorbated per unit mass of adsorbent) at equilibrium and at time 't' and is expressed in mg g^{-1}.

Pseudo-first order, pseudo-second order and intra particle diffusion models are used to describe the kinetics of MB adsorption reactions. Linear equation analysis viz; log Q_e-Q_t vs. t, t/Q_t vs. t and Q_t vs.t^(1/2) predict the validity of these models in the kinetics of adsorption reactions.

The fitting plots for pseudo-first order, pseudo-second order and intraparticle diffusion models are shown in Fig. 5, 6 and 7, respectively. Based on the values of correlation coefficients (R2) obtained from fitting results as shown in Table 6, the pseudo-first order and pseudo-second order are used as suitable models to describe the adsorption of MB onto composite I (Molybdenum dicarbonate-filter paper) and intraparticle diffusion model for the composite II

(Molybdenum dicarbonate- activated carbon). The value of k1 (min-1) for composite I and II are 0.4675 and 0.5158 respectively while as Q_e values come out as 607 and 582 (mg g-1) for these composites. However there is no concordance in the experimental and calculated Q_e values, therefore the adsorption of MB onto these composite via pseudo-first order kinetics is not wholesome. The value of Q_e, k2 and h obtained from fitting results of pseudo-second order kinetic equation for composite I and II have been found identicle and the values for these parameters are 1000 (mg g-1), 5×10-4 (min-1) and 500 mg (g min-1), respectively. These identicle values suggest the equivalent effect of Molybdenum dicarbonate on the matrices of filter paper and activated carbon.

The intraparticle diffusion model is also used to investigate the kinetics of MB onto composite I and II. The value of k_i for composite I is 165.7 g (mg min-1) and for composite II is 182.5 g (mg min-1). C_e for Composite I and II are observed as 70.53 and 57.63 mg L-1, respectively. The concordance in the experimental and calculated C_e values (50 mg L-1 and 57.63 mg L-1) in case of composite II sugests the adsorption of MB onto composite II via intraparticle diffusion model. This statement is further buttressed with good R2 value of 0.972 which is 0.963 for composite I.

3.5 Adsorption isotherm

Langmuir model 2) Freundlich model and 3) Tempkin model are used to investigate the adsorption isotherm of MB onto composite I and II. The linearalized Langmuir, Freundlich and Tempkin plots of MB adsorption by composite I and II are shown in Fig. 8, 9 and 10, respectively.

The following equation of Langmuir model is used to determine the equilibrium concentration of the adsorbate and the Langmuir adsorption constant:

$$\frac{C_e}{Q_e} = \frac{1}{K_L Q_{max}} + \frac{C_e}{Q_{max}} \quad (7)$$

Where Q_{max} is the maximum adsorption capacity at saturation (mg g-1), C_e the equilibrium concentration of the adsorbate (MB) and K_L is the Langmuir adsorption constant and that is related to the energy of adsorption.

The Langmuir adsorption isotherm parameters Q_{max} and KL calculated from the slope and intercept of the linear equations for composite I are 250 mg g-1 and 0.142 (L g-1), respectively while as these values are 250 mg g-1 and 0.111 g L-1 for composite II. R2 value for composite II is higher than composite I, suggests the adsorption of MB onto composite II via chemisorption and formation of monolayer coverage of MB on the adsorbent can be predicted. Molybdenum dicarbonate due to the presence of uncoordinated oxygen atoms binds the cationic dye via Lewis acid-Lewis base interaction thereby improves the adsorption capacity of the composite material further.

The following equaton of Freundlich model is used to determine the Freundlich adsorption constant:

$$\ln Q_e = \ln K_F + \frac{1}{n} \ln C_e \quad (8)$$

Where Q_e is the maximum adsorption capacity of adsorbent (mg g-1), C_e the equilibrium adsorbate concentration, n is the Freundlich constant, KF is the other constant related to the maximum adsorption capacity.

The following equaton of Tempkin model is used to determine the equilibrium binding energy constant:

$$Qe = B \ln KT + B \ln C_e \quad (9)$$

Where KT is the equilibrium binding energy constant and B is a constant related to the energy of adsorption.

Adsorption of MB is not restricted to Langmuir type of interactions only as R2 value for both composites I and II have been found exceeding 0.75 in Frendlich and Tempkin models. The isothermic parameters are summarized in Table 7. KF value for composite I comes out 6.16×106 and 19.68×106 for composite II. The KT values obtained after fitting the plots are also very high. This parameter is 1.12 ×106 for composite I and5.49×105 for composite II. The higher values of KF and KT for both these composites endorses the role of these models in investigating the adsorption isotherm of MB onto these composites. The hydroxyl groups of filter paper and uncoordinated lonepairs available on molybdenum dicarbonate moieties can pick up cationic MB molecules through electrostatic interactions. Such type of adsorbate and adsorbent interactions are of chemisorption natures. However the porous nature of filter paper and activated carbon components can facilitate the adsorption of MB via physiosorptions. Thus the adsorption mechanism between MB and and these composites involves both physiosorption and chemisorption phenomena.

3.6 Thermodynamic Study

The values of thermodynamic parameters like change in entropy (ΔS°), enthalpy change $(\Delta H^\circ)$and standard Gibbs free energy change (ΔG°) for the adsorption of MB from aqueous solution onto composites I and II are summarized in Table 8. The following equations (10 &11) are used to calculate these parameters.

$$\ln (Q_e/C_e) = \frac{\Delta S^\circ}{R} + -\Delta H^\circ/RT \quad (10)$$

where Q_e is the maximum adsorption capacity of adsorbents (mg g^{-1}), R is gas constant (J K^{-1} mol^{-1}) and T is the temperature. The term ln (Q_e/C_e) of Van't Hoff equation (10) is termed as adsorption affinity. Plotting ln (Q_e/C_e) vs. 1/T as shown in Fig.11, the values of ΔS° and ΔH° are obtained from the intercept and slope of the fitted line plot, respectively.

ΔG° is calculated by the following Gibbs-Helmholtz equation.

$$\Delta G^\circ = \Delta H^\circ - T\Delta S^\circ \quad (11)$$

The touchstone for a reaction to occur via physiosorption, hydrogen bonding interaction or a chemisorption is predicted and described by Rehman et al.[47]. As per the stated authors [47], the ΔH° value for physical adsorption is 4-10 KJ mol^{-1}. The ΔH° value for Hydrogen bonding forces are 2-40 KJ mol^{-1} and it is greater than 40 KJ mol^{-1} for chemical adsorption type of reactions.

The ΔH° value for adsorption of MB on composite I is 6.453 KJ mol^{-1} and onto composite II is 8.779 KJ mol^{-1}. These results suggest that the adsorbate (MB)- adsorbent interactions correspond to physiosorption type. Another standard for predicting the type of adsorption is the value of standard free energy change (ΔG°). For physical adsorption, ΔG° lies in between -20 to 0 KJ mol^{-1} and this value for chemical adsorption ranges in between -80 and -400 KJ mol^{-1} [48]. The ΔG° value for the MB adsorption onto composites I

and II also establishes the interactions between MB and adsorbents a physiosorption one and also spontaneous in the temperature range from 20 °C to 80 °C. The ΔG° values from 20 °C to 80 °C ranges from -5.994 to -8.544 KJ mol^{-1} for composite I and -6.132 to -9.085 KJ mol^{-1} for composite II.

As the value of enthalpy change (ΔH°) comes out positive, this shows the endothermic nature of the adsorption process. A positive value of entropy change (ΔS°) indicates disorderdness at the solid/liquid interface so the adsorption of MB onto these composites is an entropy driven spontaneous process and the spontaniety of the adsorption processes are further substantiated with the negative value of ΔG°. The removal of MB (per unit mass of adsorbent) from aqueous solution increases imperceptibly with increase in temperature upto 80 °C beyond which a small decrease in the removal of MB occurs as already discussed in section 3.3.5 (Effect of Temperature). This increase could be because of the enhanced thermal motion of MB molecules and a decrease in the solute solvent interaction upto 80 °C. Temperature onwards 80°C, desorption would likely to occur. Thus these adsorbents have better removal efficiency of MB from aqueous solutions upto higher temperature limit of 80 °C.

4. Conclusion:

(i) Molybdenum dicarbonate-filter paper and activated carbon composites can be used as efficient adsorbents in waste water treatment due to their high efficiency removal and adsorption capacities over a wide range of temperature. At 20 °C, composite I and II shows MB removal efficiency percentage of 87 and 96.25

(ii) The amount of MB removal increases from aqueous solution both by increasing the adsorbent dosage (100 to 500 mg) as well as the initial concentration of MB (50-80 mg L-1).

(iii) Maximum removal of MB occurs at pH 7 within 5 minutes of contact time.

(iv) Removal of MB from the aqueous solution using these composites increases with increase in temperature from 20 to 80 °C probably due to higher thermal motion of dye molecules.

(v) Adsorption of MB onto composite I conform with pseudo-first order and pseudo-second order kinetics due to good regression values of R2 whereas composite II suited well with Intraparticle diffusion model.

(vi) Adsorption of MB onto composite I aligned with Freundlich and Tempkin models due to higher regression values of R2 whereas composite II fitted well with Langmiur isothermic model.

(vii) Adsorption of MB onto composite I and II are spontaneous and endothermic.

Acknowledgements

We would like to express our gratitude to the reseach institution of Sophisticated Analytical Instrumentation Facility Sophisticated test and instrumentation centre (SAIF STIC) Kochi for providing the instrumentation facilities. The authors are thankful to two Lab. Bearers Mr. Owaise Ahamad and Mr. Sameer Khalil Dar and Head of the Department of Chemistry, GDC Anantnag, Prof Fayaz Ahmad Bhat, for their support and cooperation in accomplishing the basic expermination part of this research work.

Funding

Not applicable.

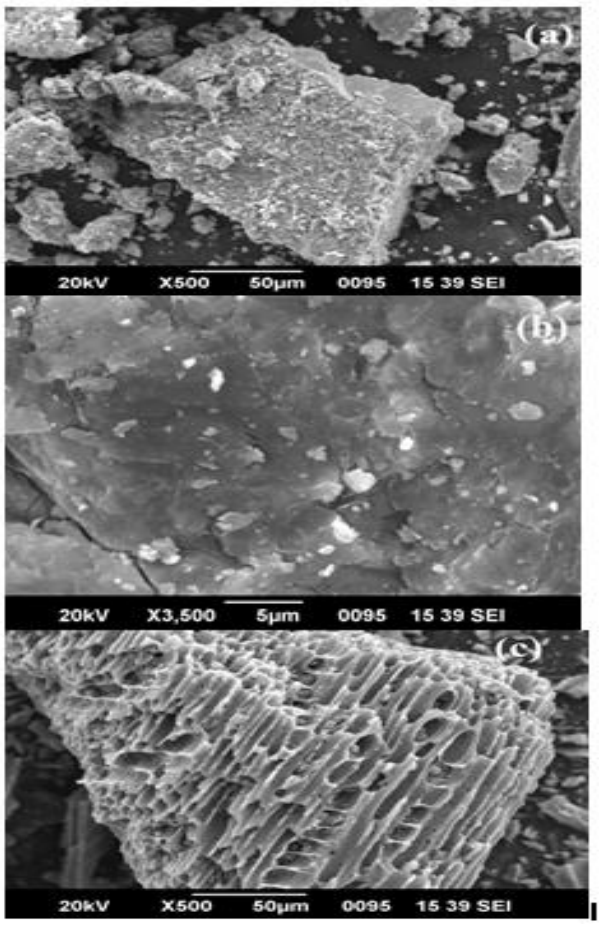

Fig 1. SEM images of (a) Molybdenum dicarbonate, (b) Molybdenum dicarbonate-filter paper and (c) Molybdenum dicarbonate-activated carbon composite.

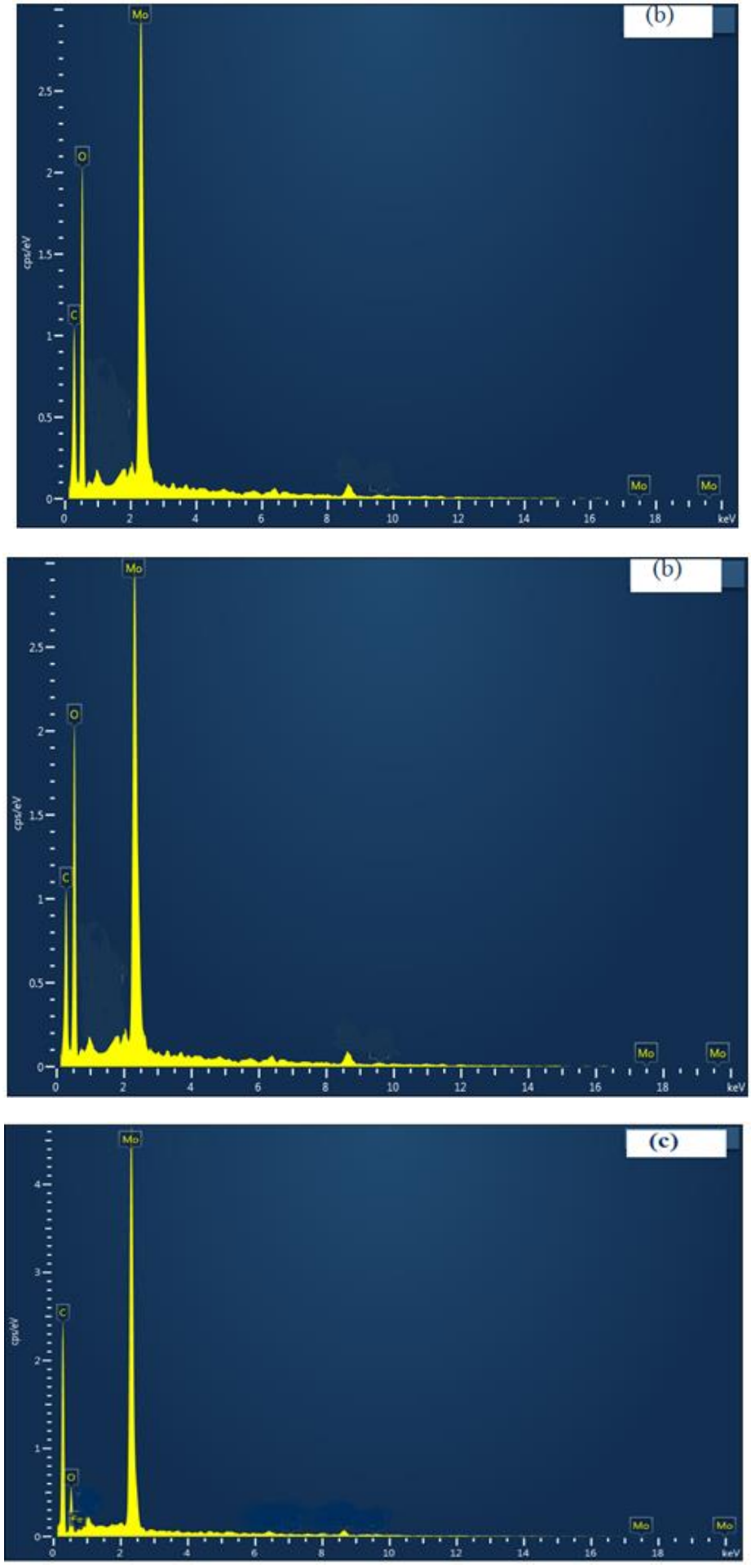

Fig 2. EDS spectrum of (a) Molybdenum dicarbonate, (b) Molybdenum dicarbonate-filter paper and (c) Molybdenum dicarbonate-activated carbon composite.

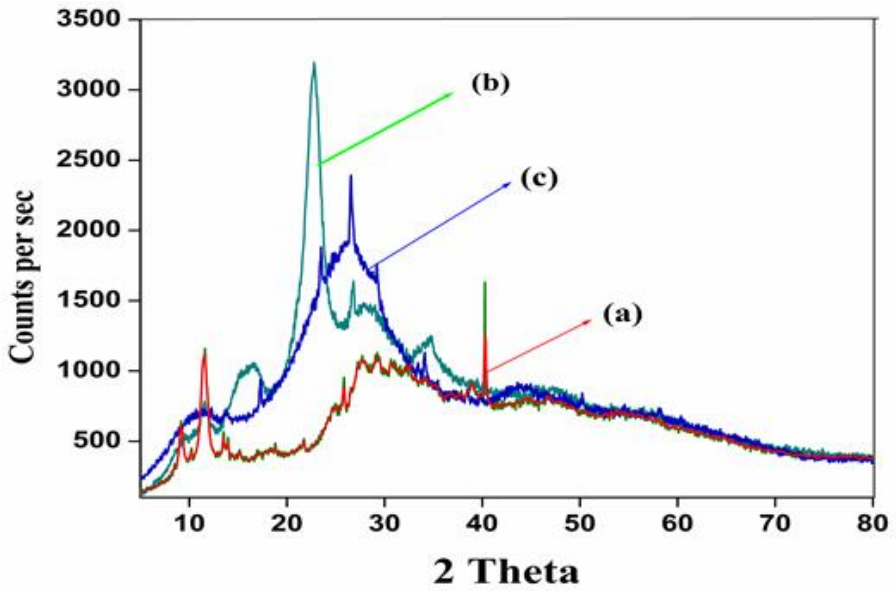

Fig 3. XRD spectrum of (a) Molybdenum dicarbonate, (b) Molybdenum dicarbonate-filter paper and (c) Molybdenum dicarbonate-activated carbon composite.

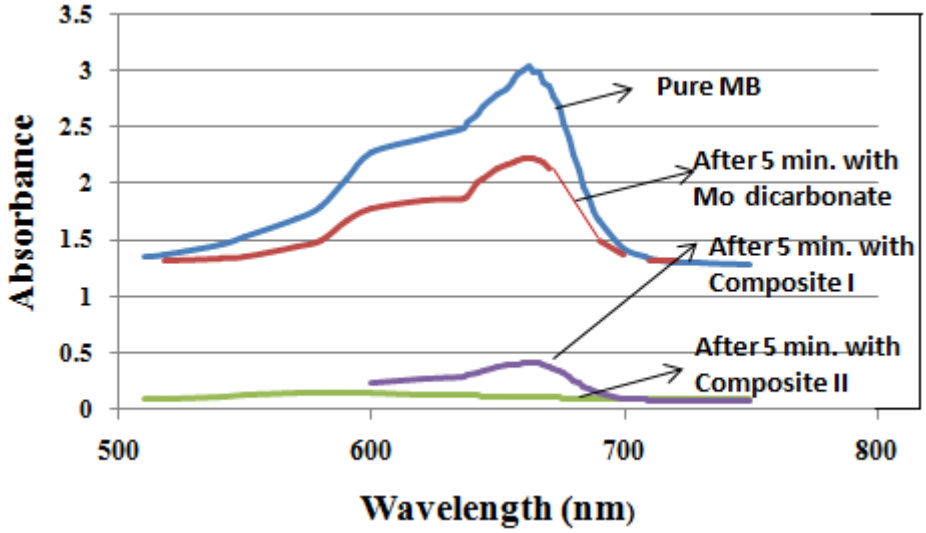

Fig 4. Visible spectra of MB aqueous solution treated with composites I and II at room temperature.

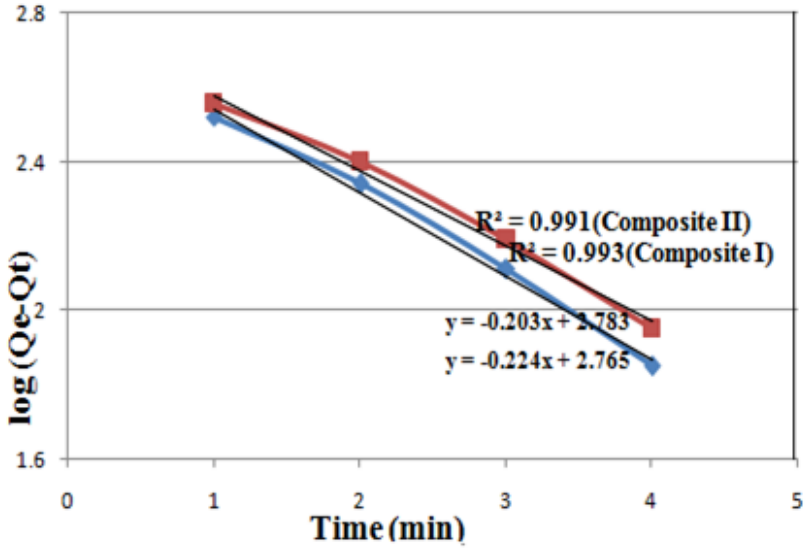

Fig 5. Pseudo-first order plot for MB adsorption by composites I and II.

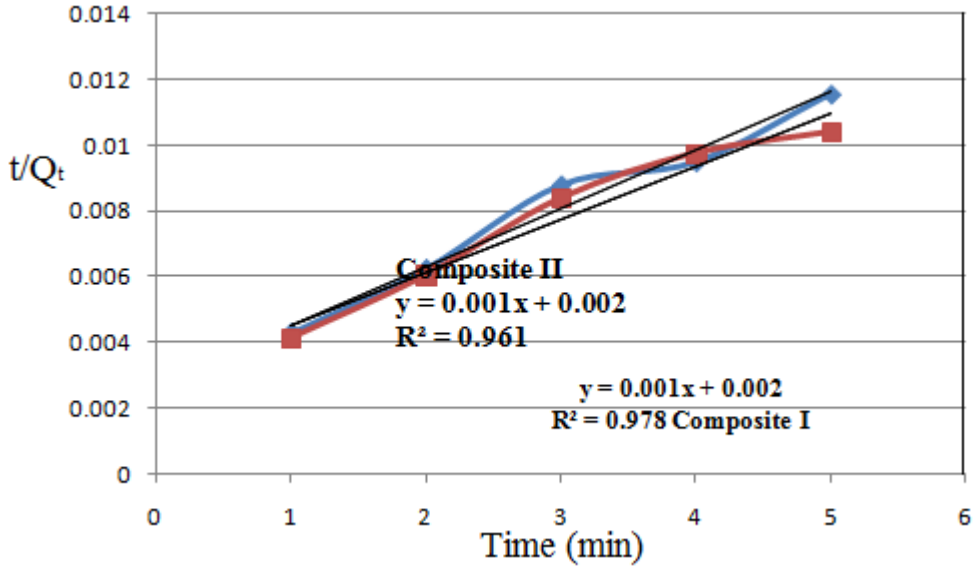

Fig 6. Pseudo-second order plot for MB adsorption by composites I and II.

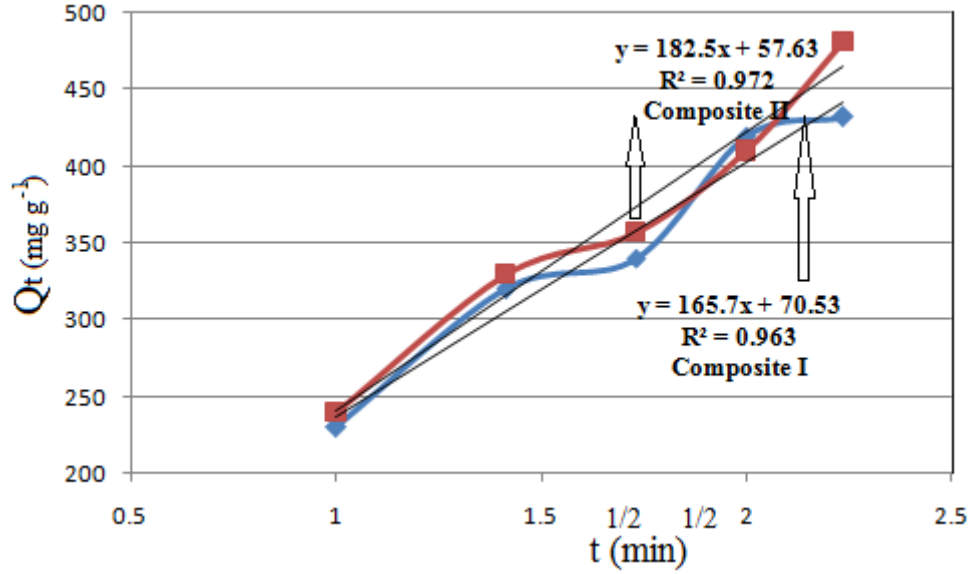

Fig 7. Intraparticle diffusion plot for MB adsorption by composites I and II.

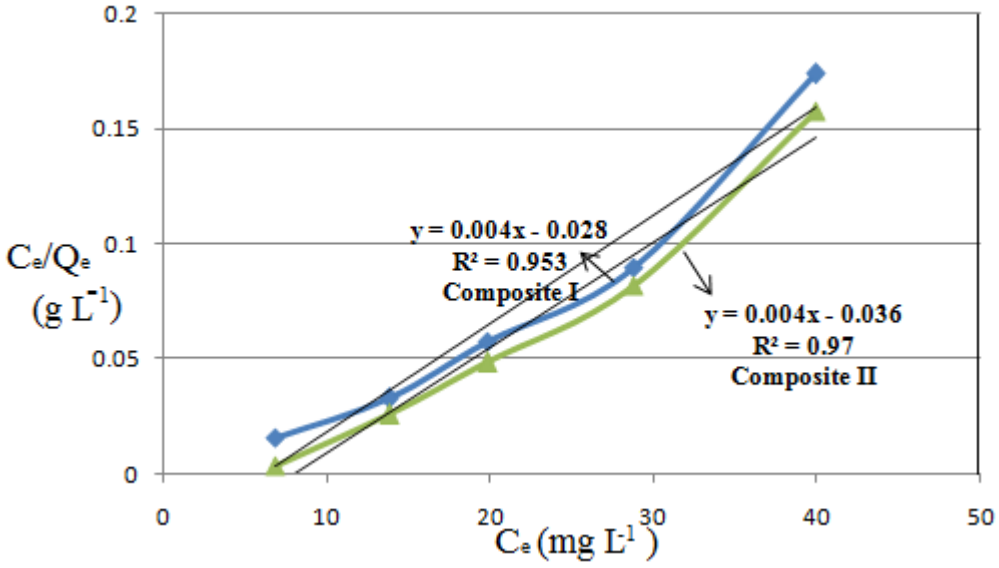

Fig 8. Langmuir isotherm plot for MB adsorption by composites I and II.

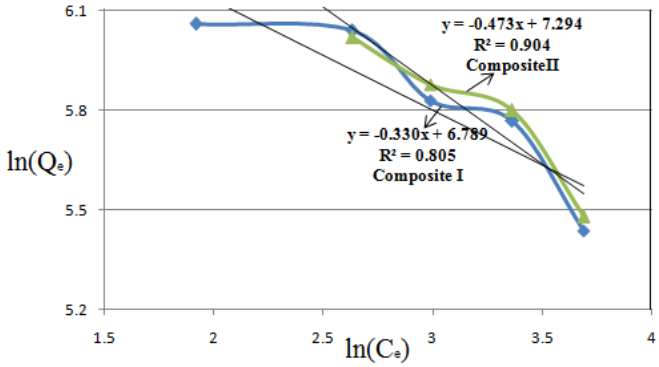

Fig 9. Freundlich isotherm plot for MB adsorption by (a) composites I and II.

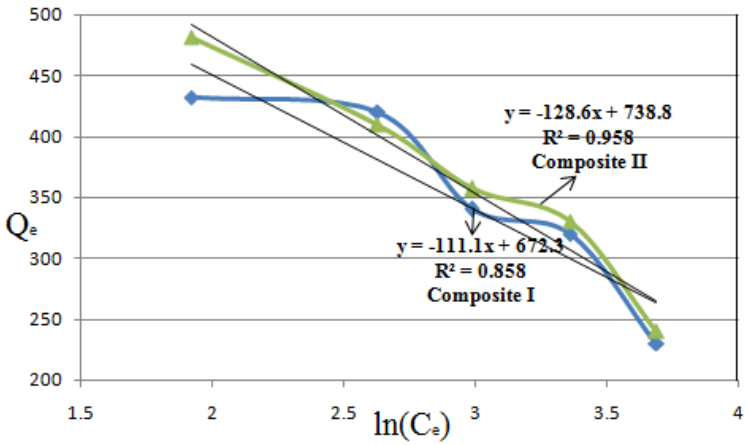

Fig 10.Tempkin isotherm plot for MB adsorption by composites I and II.

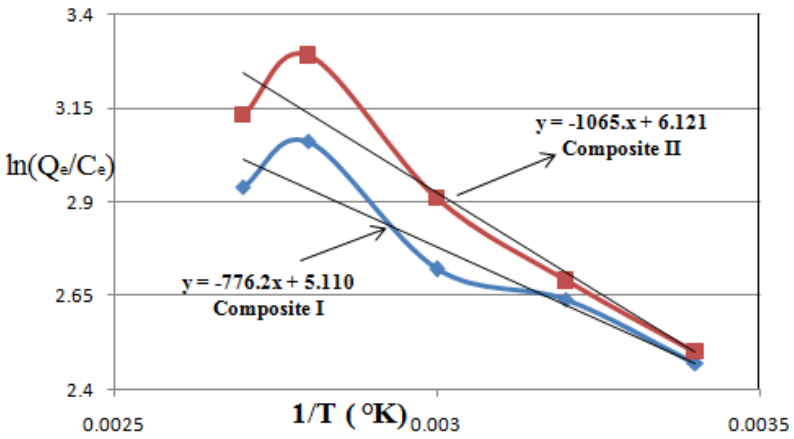

Fig 11. Plot to determine thermodynamic parameters of MB adsorption by composites I and II.

Table 1. Efficiency removal and maximum adsorption capacities of composite I and composite II towards MB

Time (min)	Maximum adsorption capacity (mg g^{-1})		Efficiency Removal (%)		Maximum adsorption capacity (mg g^{-1})		Efficiency Removal (%)	
	Filter Paper	Composite I	Filter Paper	Composite I	Activated Carbon	Composite II	Activated Carbon	Composite II
1	140	230	44	60	86	240	56	66
2	148	320	56	64	90	330	60	68
3	163	340	60	71	92	357	63	74
4	220	420	65	78	94	418	65	88
5	243	432	66	87	99	481	66	96

Table 2. Maximum adsorption capabilities for MB by different adsorbents

Adsorbents	Adsorption capability (mg g^{-1})	C_0 (mgL^{-1})	Reference
Metalloporphyrin	110.53	50	[37]
Polyaniline Magnetite composite	61.51	400	[38]
Polyaniline coated gold-aryl nanocomposite	312	480	[39]
Polypyrrole/sawdust composite	34.36	50	[40]
Graphene oxide/calcium alginate composites	182	80	[4]
Activated Carbon (Ficus Caria Bast	47.62	70	[9]
Activated Carbon (Surfactant modified)	220	50	[15]
$ZnCl_2$ activated carbon	463	50	[13]
Biomass-based activated Carbon	769	50	[2]
Graphene based Mg Silicate	592.2	50	[41]
Pinecone biomass	110	40 ($PPmL^{-1}$)	[42]
nMn-bamboo composite	322	140	[43]
Graphene-polypyrrole composite	270	100	[44]
Nickel alginate/activated carbon	505	8.3	[10]
Chitosan-g-polyacrylic acid montmorillinote composite	186	200	[23]
Black Zeolites	57.64	50	[45]
Magnetite porous carbons	306	50	[46]
PANI (Emeraldine Base)	413	50.5	[21]
PANI-Nitroprusside Composite	497	50.5	[21]
Mesoporous Carbons (Peach Stones)	444	200	[6]
Molybdenum dicarbonate	135	50	[Present study]
Molybdenum dicarbonate- filter paper composite	432	50	[Present study]
Molybdenum dicarbonate- activated carbon	481	50	[Present study]

Table 3. Effect of initial concentration (C_0) of MB on the adsorption by Composite I and Composite II

C_0 (mg L^{-1})	50	60	70	80
Adsorbent	Adsorption %			
Composite I	87.00	84.14	81.45	77.30
	96.25			
Composite II		95.23	94.37	91.20

Table 4. Effects of solution pH on adsorption percentage of MB onto composite I and composite II

pH	2	4	7	10	12
Composite I	65.20	72.12	87.00	76.24	75.12
Composite II	75.34	85.17	96.25	80.60	78.14

Table 5. Effects of Temperature on the adsorption of MB onto composite I and composite II

Adsorption capacity (mg g^{-1})	Temperature				
	20°C	40°C	60°C	80°C	100°C
Composite I	432	435	440	443	388
Composite II	481	485	489	494	394

Table 6. Kinetic Parameters for MB adsorption by composite I and II.

Materials	Type	Parameters		
	Pseudo-first order kinetics	**k_1(min^{-1})**	**Q_e(mgg^{-1})**	**R^2**
Composite I		0.4675	607	0.991
Composite II		0.5158	582	0.993
	Pseudo-second order kinetics	k_2 (min^{-1})	Q_e(mgg^{-1})	R^2
Composite I		5×10^{-4}	1000	0.978
Composite II		5×10^{-4}	1000	0.961
	Intra-particle diffusion model	k_i(g (mg min^{-1})	C_e (mgL^{-1})	R^2
Composite I		165.7	70.53	0.963
Composite II		182.5	57.63	0.972

Table 7. Parameter values of different adsorption models (calculated after linear fit method).

Materials	Langmuir Model			Freundlich		Tempkin	
	Q_{max}	K_L	R^2	K_F (Lg^{-1})	R^2	K_T(Lmg^{-1})	R^2
Composite I	250	0.142	0.953	6.16×10^6	0.805	1.12×10^6	0.858
Composite II	250	0.111	0.97	19.68×10^6	0.904	5.49×10^5	0.958

Table 8. Thermodynamic parameters for the removal of MB by composites I and II

Adsorbent	ΔG° (J mol^{-1})				ΔH° (J mol^{-1})	ΔS° (J K^{-1} mol^{-1})
	20°C	**40°C**	**60°C**	**80°C**		
Composite I	-5994	-6418	-7693	-8542	6453	42.48
Composite II	-6132	-7149	-8167	-9085	8779	50.89

5. References

[1] Freshwater Resources, National Geographic Society " education.nationalgeographic.org.

[2] N U M. Nizam NUM, M. M. Hanafiah MM, E. Mahmoudi E, A. A. Halim AA and A. W. Mohammad AW, 2021, Scientific Reports, 11 (2021) 8623-8640.

[3] E. Okoniewska E, Sustainability, 13 (2021) 4300-4312.

[4] Y. Li Y, Q. Du Q, T. Liu T, J. Sun J, Y. Wang Y, S. Wu S, Z. Wang Z, Y. Xia Y, L. Xia L, 2013, Carbohydrate Polymers 95 (2013) 501– 507.

[5] Abate et al. 2020, Environmental System Research, 9 (2020) 29-42.

[6] S. Álvarez-Torrellas S, R. García-Loverab R, A. Rodrígueza A, J. García J, 2015, Chemical Engineering Transactions, 43 (2015) 1963-1968.

[7] P. R. Evora PR and F. Viaro F, (2006), Curr Drug Targets, 7(9) (2006) 1195-204.

[8] P. R. Evora PR et al (2015), Rev Bras Cir Cardiovasc. 30(1) (2015) 84-92.

[9] D. Pathania D, S. Sharma S, P. Singh P, Arabian Journal of Chemistry, (2013)1-7. http://dx.doi.org/10.1016/j.arabjc.2013.04.021.

[10] Y. Wang Y, J. Pan J, Y. Li Y, P. Zhang P, M. Li M, H. Zheng H, X. Zhang X, H. Li H and Q. Du Q, Journal of Material Research and Technology, 9(6) (2020) 12443–12460.

[11] T. Etemadinia T, A. Allahrasani A and B. Barikbin B, Polymer Bulletin, 76(12) (2019) 6089-6109.

[12] S. N. Hurairah SN, N. M. Lajis NM, A. A. Halim AA, Journal of Geoscience and Environment Protection, 2020, 8, 128-143.

[13] M. Khodaie M, N. Ghasemi N, B. Moradi B and M. Rahimi M, Journal of Chemistry, (2013)1-6. http://dx.doi.org/10.1155/2013/383985.

[14] P. K. Malik PK, Journal of Hazardous Materials B113 (2004) 81–88.

[15] Y. Kuang Y , X. Zhang X and S. Zhou S, Water, 12 (2020) 587-605.

[16] Jayachandran Sheeja J, Krishnan Sampath K and Ramasamy Kesavasamy R, Adsorption Science and Technology, (2021) 1-12. https://doi.org/10.1155/2021/5035539.

[17] M. Stan M et al. Synthetic Metals, 288 (2022) 117117.

[18] S. Karthi S, R. K. Sargeetha RK, K. Arumugam K, T. Karthitta T and S. Umala S, Materials Today: Proceedings, 66(4) (2022) 1945-1950.

[19] W-D Xiao WD et al. International Journal of Biological Macromolecules, 218 (2022) 285-294.

[20] H. Li H, V. L. Budarin VL, J. H. Clark JH, M. Noth M and X. Wu X, Journal of Hazardous Materials, 436 (2022) 129174.

[21] F. A. Rafiqi FA and K. Majid K, Journal of Material Sciences, 52(11) (2017) 6506-6524.

[22] F. A. Rafiqi FA and K. Majid K, Journal of Environmental Chemical Engineering, 3(4) (2015) 2492-2501.

[23] L. Wang L, J. Zhang J, A. Wang A, Colloids and Surfaces A: Physicochemical and Engineering aspects, 322 (2008) 47-53.
[24] J. Yan J and R. Xu R, Bioresources, 10 (2015) 4065-4076.
[25] A.M. Youssef AM, S. Kamel S, M. El-Sakhawy M, M.A. E Samahy MAE, Carbohydrate Polymers, 90 (2012) 1003–1007.
[26] M. Liu M, S. He S, W. Fan W, Miao Yue-E and T. Liu T, Composites Science and Technology,101 (2014) 152–158.
[27] T. K. Sen TK, S. Afroze S, H. M. Ang HM, Water Air Soil Pollution, 218 (2011) 499.
[28] S. Zhou S et al. Carbohydrate Polymers, 258(2021) 117690-117699.
[29] H. Bian H, Y. Yang Y and P. Tu P, Bioresources, 16(4) (2021) 8353-8365.
[30] X. Li X, W. Liu W, Mengjuan Li M, Y. Li Y, Mi. Ge M, Polymer Composites, 35 (2014) 993-998.
[31] H. A. Hamid HA et al. Progress in Engineering Applications and Technology, 1(2020) 116-126.
[32] A. Szyman´ska A, W. Nitek W, M. Oszajca M, W. Łasocha W, K. Pamin K and J. Połtowicz J, CatalLett, 146 (2016) 998–1010.
[33] R. K. Dev RK, A. Bhattarai A, N. K. Chaudhary NK and P. Mishra P, Int. J. Pharm. Sci. Rev. Res.,60(1) (2020) 115-121.
[34] R.B. Rastogi RB and M. Yadav M, Tribology International 36 (2003) 511–516.
[35]https://en.m.wikipedia.org/wiki/Ammonium tetrathiomolybdate.
[36] H. N. Abdelhamid HN, A. P. Mathew AP, Carbohydrate Polymers, 274 (2021) 118657-63.
[37] M. M. Almoneef MM, J. Roubeh J and M. Mbarek M, Synthetic Metals, 290 (2022) 117158.
[38] D. D. A. Buelvas DDA et al. Synthetic Metals, 292 (2023) 117232.
[39] B. A. AlMashrea BA et al. Synthetic Metals, 269 (2020) 116528-116540.
[40] R. Ansari R, Z. Mosayebzadeh Z, Journal of the Iranian Chemical Society, 7 (2010) 339-350.
[41] A. Que, T. Zhu & Y. Zheng, J Mater Sci 56, (2021) 16351–16361.
[42] J. D. Xiao JD, L. G. Qiu LG, X. Jiang X, Y. J. Zhu YJ, S. Ye S, X. Jiang X, Carbon, 59 (2013) 372.
[43] S. E. Shaibu SE, F. A. Adekola FA, H. I. Adegoke HI, O. S. Ayanda OS, Materials, 7 (2014) 4493-4507.
[44] L. Bai L, Z. Li Z, Y. Zhang Y, T. Wang T, R. Lu R, W. Zhou W, H. Gao H, S. Zhang S, Chemical Engineering Journal, 279 (2015) 757-766.
[45] M. M. Selim, D.M. EL-Mekkawi, F. A. Ibrahim, J. Mater Sci, 53 (2018) 3323-3331.
[46] J. D. Xiao JD et al. Carbon, 59 (2013) 372-382.
[47] L. Bai L et al., Chemical Engineering Journal, 279 (2015) 757-766.
[48] W. Wang W et al., Applied Surface Science, 346 (2015) 348-353.